

1 **Vacuolar invertase knockout enhances drought tolerance in potato plants**

2

3 Marina Roitman^{1,2}, Paula Teper-Bamnolker¹, Adi Doron-Faigenboim³, Noga Sikron⁴,

4 Aaron Fait⁴, Ondrej Vrobel^{5,6,7}, Petr Tarkowski^{5,6}, Menachem Moshelion², Samuel

5 Bocobza³ and Dani Eshel¹

6

7 ¹ Department of Postharvest Science, Agricultural Research Organization – Volcani

8 Institute, Rishon LeZion, Israel

9 ² Institute of Plant Sciences and Genetics in Agriculture, The Robert H. Smith Faculty

10 of Agriculture, Food and Environment, The Hebrew University of Jerusalem,

11 Rehovot, Israel

12 ³ Institute of Plant Sciences, Agricultural Research Organization – Volcani Institute,

13 Rishon LeZion, Israel

14 ⁴ The Jacob Blaustein Institutes for Desert Research, Ben-Gurion University of the

15 Negev, Midreshet Ben-Gurion, Israel

16 ⁵ Czech Advanced Technology and Research Institute (CATRIN), Palacký University,

17 Olomouc, Czechia

18 ⁶ Czech Agrifood Research Center, Genetic Resources of Vegetables and Special

19 Crops, Olomouc, Czechia

20 ⁷ Department of Biochemistry, Faculty of Science, Palacký University, Olomouc,

21 Czechia

22 **Abstract**

23 Drought stress is one of the most critical abiotic constraints limiting crop productivity
24 worldwide, exacerbated by ongoing climate change and increasingly frequent extreme
25 weather events. Stomatal regulation and osmoprotective sugar accumulation are critical
26 adaptive mechanisms for plant survival under drought stress. Here, we characterize the
27 enhanced drought resilience observed in CRISPR/Cas9-mediated potato, mutants in
28 their vacuolar invertase gene (*StInv*). Knockout plants exhibited improved
29 performance under progressive drought stress and during rewatering drought,
30 maintaining higher stomatal conductance, elevated transpiration rates, and superior
31 photosynthetic efficiency compared to wild-type (WT) plants. These improved
32 performance under similar transpiration rate led to higher agronomic water-use
33 efficiency (AWUE) in *stinv* plants resulting in greater biomass production despite
34 reduced water availability. Metabolomic profiling revealed distinct adaptive strategies;
35 *stinv* plants preferentially accumulated galactinol and raffinose, indicating enhanced
36 raffinose family oligosaccharide (RFO) metabolism. Furthermore, *stinv* plants
37 displayed lower levels of abscisic acid (ABA) and its catabolites under drought,
38 suggesting a moderated ABA response facilitating a more risk-taking growth strategy
39 that supports sustained growth and physiological stability. Our findings identify
40 targeted metabolic and hormonal adjustments underlying drought resilience in potato
41 plant, offering promising strategies for enhancing crop performance under water-
42 limited conditions.

43

44 **Introduction**

45 Abiotic stresses impair plant growth and development, reduce productivity, and limit
46 plant species' geographical distribution [1]. Plants' survival depends on their timely and

47 pertinent responses to changes in growth conditions, the severity and duration of stress
48 conditions, and the capacity to adapt quickly to changing energy equations [2]. Plants
49 cope with abiotic stress by differentially regulating various genes at the transcriptional
50 level [reviewed by 3]. These stress-responsive genes play a role in stress-signal
51 transduction and gene-expression regulation; the products from these genes protect
52 plant cells from stress-related damage and maintain cell viability [4]. The antioxidant
53 defense machinery protects plants against oxidative stress damage [5]. Plants possess
54 efficient enzymatic and non-enzymatic antioxidant defense systems. These systems
55 work in concert to control the cascades of uncontrolled oxidation and protect plant cells
56 from oxidative damage by scavenging of reactive oxygen species (ROS) [6, 7].

57 Osmotic adjustment is an effective component of stress tolerance. Accumulation of
58 osmoprotectants (proline, glycine betaine, gamma-aminobutyric acid, and sugars) is a
59 typical response to abiotic stresses observed in different plant systems [8]. Modulating
60 the expression of genes related to the production and accumulation of compatible
61 solutes helps plants to tolerate osmotic stress by maintaining water potential and
62 protecting cellular organelles and essential proteins [9]. Soluble sugars are important
63 osmoprotectants that play a significant role in cellular osmotic adjustment by protecting
64 cell structures exposed to environmental stress [10-13]. Sucrose and sucrosyl
65 oligosaccharides, including fructans and RFOs, accumulate in the vacuoles under
66 oxidative stress as a consequence of abiotic stress, protecting the tonoplast against
67 ROS-mediated damage [14]. During stress, sucrose and RFOs can be transported from
68 the vacuole to the apoplast as tonoplast exocytosis vesicles for stabilization of cell
69 membrane [15, 16].

70 Sucrose and its cleavage products glucose and fructose are central molecules for cellular
71 biosynthesis and signal transduction throughout the plant life cycle [17]. Sucrose may
72 serve as a protectant against cold stress by acting as a signal or as an osmoprotectant
73 (cryoprotective) molecule [16, 18]. *In-vitro* studies have shown that the ID₅₀ value
74 required to inhibit OH⁻ catalyzed hydroxylation by sucrose is similar to that of
75 glutathione antioxidant [19]. In agreement with this, PpINH1, an invertase inhibitor in
76 peach, maintains high sucrose levels, improves membrane stability during cold storage,
77 and enhances resistance to chilling injury [20, 21].

78 Other essential water-soluble carbohydrates derived from sucrose include the RFOs (α -
79 galactosyl extensions of sucrose) produced by galactinol synthase (GolS) and raffinose
80 synthase (RafS) using sucrose and myo-inositol as substrates. RFOs are proposed to
81 play an essential role in protecting plants from oxidative stress, as they accumulate
82 under stressful conditions [19, 22-24]. In addition to functioning as osmolytes, RFOs
83 also participate in carbon storage, in stress signaling pathways, in membrane protection
84 and as antioxidants against ROS in different cell compartments [16, 19, 25-27].

85 Accordingly, inhibition of the *VACUOLAR INVERTASE* gene (VInv) in *Arabidopsis*
86 *thaliana* or *Solanum tuberosum* promoted accumulation of raffinose, increasing the
87 cold tolerance of transgenic plants [28, 29]. Generally, rice (*Oryza sativa*) and
88 *Arabidopsis* do not accumulate large quantities of RFOs in tissues under optimal
89 conditions. However, RafS accumulation was observed under stressed conditions, such
90 as extreme temperature [30, 31]. Although there is evidence of a correlation between
91 GolS activity and RFOs content, the concentration of the initial substrates (myo-inositol
92 and sucrose) is the key for RFOs accumulation at least in seeds and tubers [29, 32-34].
93 Sucrosyl oligosaccharides and the enzymes associated with their metabolism may

94 interact indirectly with ROS-signaling pathways [27, 35]. In addition, RFOs and
95 galactinol have been proposed to play important roles in oxidative-stress protection in
96 plants during stress acclimation [15, 19, 36]. All these previous studies show that the
97 production of sugars is beneficial for plant survival during abiotic stress.

98 A previous review suggests that ROS signaling interacts with ABA, Ca²⁺ fluxes, and
99 sugar sensing, and may function both upstream and downstream of ABA-dependent
100 pathways during drought stress [37]. This has implied that RFOs may play a pivotal
101 role in the initial adaptation of plants to water-deficient conditions, potentially by
102 controlling both ROS signaling and metabolism [16, 38]. Plant's responses to drought
103 stress are closely linked to the hormone ABA [39]. Drought-related gene expressions
104 are believed to be governed through both ABA-dependent and ABA-independent
105 mechanisms [40]. Numerous elements of the ABA signaling pathway and the control
106 of gene expression downstream of ABA signaling have been thoroughly documented,
107 but the ABA-independent pathway remains elusive and not well understood [41]. When
108 plants experience stress, the production of ABA from scratch relies on the activation of
109 the *NCED3* gene [42]. This gene codes for a 9-cis-epoxycarotenoid dioxygenase
110 enzyme, which plays a crucial role in the primary step of ABA biosynthesis. In
111 situations where roots face water scarcity, a hydraulic signal is generated, leading to a
112 swift transmission of a water deficiency signal from the roots to the leaves of the plant.
113 This, in turn, initiates the synthesis of ABA in the leaves and the closing of stomata
114 [43].

115 In the study of the ABA biosynthesis mutant *nced3* subjected to dehydration stress,
116 researchers observed that proline (an amino acid involved in plant stress response),
117 branched-chain amino acids (BCAAs), and gamma-aminobutyric acid (GABA)

118 accumulate later and in lower quantities compared to sugars, and this pattern was
119 influenced by the presence of ABA. On the other hand, RFOs and the antioxidant
120 ascorbate increased independently of ABA [44]. These results suggest that the ABA-
121 independent response to drought likely occurs earlier than the ABA-dependent response
122 [38].

123 Drought stress poses a major challenge to the production of potatoes worldwide.
124 Climate change is predicted to further aggravate this challenge by intensifying potato
125 crop exposure to increased drought severity and frequency [45]. Drought stress was
126 reported to trigger the accumulation of soluble sugars in sink leaves of potato plants,
127 reduction in tuber number and yield and affect carbon partitioning in the whole plant
128 [45, 46]. Although the application of exogenous ABA has confirmed the ABA-induced
129 expression of stress-related genes, several drought-induced genes are insensitive to
130 exogenous ABA application [45]. The Mechanism of ABA-independent drought
131 response pathway has not been described, to our knowledge, in any plant species. We
132 are proposing to elucidate an ABA-independent pathway for drought tolerance in
133 potato. Although potato has not been a classical model for molecular biology and
134 genomics research until recently [47, 48], it provides an ideal “case study” to dissect
135 the ABA-independent drought response pathway and determine its effect on
136 agricultural crop performance.

137 The potato tuber is a swollen underground stem formed by swelling of the subapical
138 underground stolons [49]. Exposing the potato tuber to chilling during field-growth or
139 postharvest storage triggers cold-induced sweetening (CIS), characterized by the
140 accumulation of hexoses, such as glucose and fructose, mainly in the tuber parenchyma
141 [50, 51]. Accordingly, potato tubers have been shown to produce free radicals under
142 low-temperature conditions [52]. Sucrose is cleaved to hexoses by two main enzymes:

143 sucrose synthase (EC 2.4.1.13) and invertase (EC 3.2.1.26). Sucrose synthase catalyzes
144 the reversible conversion of sucrose to uridine diphosphate-glucose and fructose.
145 Invertases irreversibly split sucrose into glucose and fructose [reviewed by 53]. Sucrose
146 hydrolysis by *S. tuberosum* vacuolar invertase (StVInv) has been reported to be the
147 main pathway involved in potato CIS [54-56]. In a previous study, we demonstrated
148 that potato plants with CRISPR knocked-out *StVInv* genes (*StVInv*) exhibit enhanced
149 tolerance to combined cold and drought stress, associated with increased RFO
150 accumulation in tubers [29]. Here, we dissected the specific contributions of the *StVInv*
151 gene to drought tolerance. Using comprehensive physiological phenotyping, including
152 continuous transpiration and stomatal conductance measurements, alongside detailed
153 metabolomic analyses, we characterized the unique drought adaptation strategies of
154 *stvinv* plants. Our findings revealed that these knockout plants exhibit enhanced drought
155 resilience through sustained stomatal function, moderated ABA signaling, and a distinct
156 metabolic shift toward increased osmoprotective sugar accumulation. These findings
157 underscore the central role of sucrose metabolism in plant drought adaptation,
158 providing valuable targets for breeding drought-resilient crops.

159

160 **Results**

161 **Enhanced drought tolerance in *stvinv* plants.** We previously demonstrated the
162 enhanced tolerance of two independent CRISPR/Cas9 knockout lines of *StVInv*,
163 referred to as *stvinv-7* and *stvinv-8* potato plants to combined cold and drought stress
164 during early seedling stages (Teper-Bamnlker et al., 2023). To isolate the specific
165 effects of drought stress and elucidate the underlying mechanisms of drought response
166 in *stvinv* plants, we used one-month-old seedlings. Plants were grown under controlled
167 conditions, exposed to prolonged terminal drought followed by rehydration to assess

168 recovery, and their response was visually scored on a qualitative phenotypic scale from
169 low to high vigor. In all tested lines, the phenotype score began to decline
170 approximately 14 days after irrigation was stopped (Fig. 1A). Throughout the drought
171 period, *stvinv* plants exhibited significantly greater tolerance compared to WT plants,
172 as evidenced by higher phenotypic scores (Fig. 1A, B). Chlorophyll content was higher
173 in *stvinv* plants during the irrigation phase and the early days of drought, as well as
174 during the initial recovery period, suggesting enhanced photosynthetic efficiency
175 compared to WT plants (Fig. 1C). *stvinv* plants maintained elevated leaf stomatal
176 conductance relative to WT throughout all phases—irrigation, drought, and recovery.
177 Notably, both *stvinv-7* and *stvinv-8* exhibited significantly higher stomatal conductance
178 during severe drought and recovery (Fig. 1D). This enhanced gas exchange capacity
179 likely facilitated sustained photosynthetic activity, improved water-use efficiency, and
180 expedited recovery following drought stress.

181 **Drought tolerance of *stvinv* plants is independent of stomatal density.** To assess
182 whether the different drought response in *stvinv* plants is associated with stomatal traits,
183 stomatal density and aperture width were analyzed. Young, fully expanded leaves were
184 tested at mid-morning under controlled long-day photoperiod conditions. Imprints of
185 abaxial and adaxial leaf surfaces were made following the protocol described by Geisler
186 and Sack [57]. Microscopic analysis revealed no significant differences in stomatal
187 density or indices between *stvinv* and WT leaves across all examined surfaces, abaxial
188 and adaxial (Fig. 1E, F). Measurements showed no significant differences between WT
189 and *stvinv* leaves on both abaxial and adaxial leaf surfaces (Fig. 1F). These findings
190 indicate that the enhanced drought tolerance observed in *stvinv* plants is not attributable
191 to changes in stomatal density or aperture size.

192 ***stvinv* plants demonstrate higher transpiration rate.** To elucidate the physiological
193 water relations mechanisms underpinning drought response, whole-plant continuous
194 transpiration measurements were conducted using the high-throughput telemetric,
195 gravimetric-based phenotyping system (Fig. 2A; Plantarray 3.0, Plant-DiTech, Israel;
196 [58]). This method provided real-time, high-resolution data on water dynamics,
197 facilitating a detailed analysis of transpiration behavior during drought stress and
198 recovery in *stvinv* plants. Two-month-old plants were subjected to a controlled
199 irrigation regime consisting of three phases: an initial well-watered phase (days 1–12)
200 with excessive irrigation, a standardize drought phase (days 13–27) during which daily
201 irrigation was gradually reduced to 80% of each plant’s transpiration from the previous
202 day (enabling similar drought stress to all plants), and a recovery phase (days 28–34)
203 with resumed full irrigation.

204 During this assay, WT plants began showing visible wilting symptoms on day 21, eight
205 days after irrigation was stopped, and exhibited severe wilting by day 27. In contrast,
206 *stvinv* lines maintained higher phenotypic scores during the late drought phase (days
207 21–27), with significantly milder stress symptoms (Fig. 2B and C). Following
208 rehydration on day 27, both *stvinv* and WT plants start to recover within 24 h (Fig. 2D).

209 Also, during the well-watered phase (days 1–12), plants exhibited similar transpiration
210 rates, with *stvinv-7* plants generally trending higher (Fig. 2D). Under drought conditions
211 (days 13–27), WT plants experienced a significant decline in transpiration rates,
212 particularly between days 19–26. In contrast, *stvinv* lines maintained substantially
213 higher transpiration rates throughout this phase (Fig. 2D). During recovery from
214 drought (days 28–34), both *stvinv* lines, particularly *stvinv-8*, demonstrated
215 significantly higher transpiration rates than WT plants, highlighting their rapid
216 resilience (water-use resumption post-rehydration; Fig. 2D). Midday whole-canopy

217 conductance measurements (10:00–15:00) confirmed that *stvinv* plants consistently
218 maintained higher conductance levels under drought stress compared to WT plants (Fig.
219 S1). This higher gas exchange capacity reflects their ability to regulate water loss while
220 sustaining physiological functions. Additionally, normalized transpiration rates
221 (calculated as transpiration relative to biomass) further underscored the drought
222 resilience of *stvinv* plants, with significantly higher rates during both the drought and
223 recovery phases (Fig. 2E).

224 Whole-canopy transpiration rates, normalized to biomass (E), highlight consistently
225 higher transpiration levels in *stvinv* plants compared to WT plants under drought
226 conditions (Fig. 3A). On peak drought days (e.g., day 23), E measured during daylight
227 hours (06:00–18:00) provided insights into stomatal dynamics. Normalizing the
228 transpiration rate to VPD, revealed that *stvinv* plants exhibited consistently elevated
229 midday conductance (Fig. 3C) and transpiration (Fig. 3B), without temporal variation,
230 indicating a stable, robust drought adaptation strategy. This stable, ‘risk taking’,
231 transpiration behavior suggests more carbon fixation and evaporative cooling,
232 contributing to the enhanced drought resilience of *stvinv* plants.

233 ***stvinv* plants present a better water-use efficiency.** Soil moisture thresholds (Θ_{crit})
234 at which plants restricted transpiration were determined to evaluate the whole plant
235 water balance regulation. WT plants began restricting transpiration at higher soil
236 moisture levels ($\Theta_{crit} = 0.14 \text{ cm}^3/\text{cm}^3$) compared to *stvinv* plants ($\Theta_{crit} = 0.12$
237 cm^3/cm^3 for *stvinv-7* and $0.09 \text{ cm}^3/\text{cm}^3$ for *stvinv-8*) (Fig. 3E). This gradual response to
238 soil drying in *stvinv* plants enabled sustained transpiration, improving their ability to
239 utilize available water efficiently during prolonged drought.

240 Both *stvinv-7* and *stvinv-8* lines demonstrated significantly higher AWUE compared to
241 WT plants, as calculated by the ratio of shoot dry biomass to total transpired water (Fig.
242 3F). *stvinv-8* exhibited the highest AWUE values, indicating superior biomass
243 production per unit of water consumed. These results suggest that *stvinv* plants utilize
244 a better water use efficiently under drought conditions.

245 ***stvinv* plants exhibit enhanced biomass production following drought stress.** To
246 assess whether the drought tolerance of *stvinv* plants translates into improved growth
247 and productivity, shoot, root, and tuber parameters were evaluated at the conclusion of
248 the 35-day experiment. *stvinv* plants, particularly *stvinv-8*, demonstrated significantly
249 higher shoot dry weight compared to WT plants, reflecting enhanced biomass
250 accumulation under stress conditions (Fig. 4A). Root length measurements showed no
251 significant differences among genotypes, indicating that drought tolerance in *stvinv*
252 plants is not linked to root elongation (Fig. 4B). Additionally, the *stvinv-7* line produced
253 a slightly higher number of tubers compared to WT and *stvinv-8* (Fig. 4C). These
254 findings demonstrate that *stvinv* plants not only exhibit drought tolerance but also
255 effectively convert this resilience into enhanced shoot biomass, underscoring their
256 potential for improved growth in water-deficient conditions.

257 ***stvinv* plants display enhanced osmoprotection and lower stress perception under**
258 **drought.** To investigate the metabolic adaptations associated with the *StVInv* knockout
259 and its potential role in drought tolerance, we performed a comprehensive metabolomic
260 profiling. Fully expanded young leaves from the third node below the apical bud were
261 sampled at five time points: baseline (T0, following 10 days of irrigation); mild drought
262 (T1, T2; after 7 and 9 days without irrigation); progressive drought stress (T3, T4; after
263 12 and 14 days without irrigation); and recovery (T5, one day post-rewatering).
264 Samples were analyzed using gas chromatography mass spectrometry (GC-MS) for

265 untargeted metabolomic profiling. Metabolite analysis revealed that WT plants
266 displayed greater level of homoserine and shikimic acid, which are markers of
267 intensified amino acid and secondary metabolism, following drought stress (Fig. 5A).
268 *stvinv* plants consistently accumulated significantly higher levels of osmoprotective
269 sugars such as galactinol and raffinose (Fig. 5B), indicating the distinct stress response
270 strategies between genotypes.

271 Pathway enrichment analysis confirmed this divergence: WT plants exhibited broad
272 activation of stress-related pathways including glycine, serine, threonine and galactose
273 metabolism and amino acid biosynthesis (Fig. S2), whereas *stvinv* plants showed
274 similar pattern but in higher levels of galactose and sucrose metabolism and unique
275 glyoxylate/dicarboxylate higher metabolism (Fig. S2). This metabolic adjustment in
276 *stvinv* lines appears more energy-efficient, prioritizing carbon conservation and
277 osmoprotection over protein turnover. Notably, this efficiency is further enhanced by
278 increased activation of glyoxylate and dicarboxylate metabolism, facilitating carbon
279 conservation and maintaining energy balance under drought stress. Additionally,
280 elevated citric acid levels in *stvinv* plants point to a more efficient TCA cycle, providing
281 sufficient ATP to support cellular functions during water deficit. Correlation heatmaps
282 further highlighted these differences, showing a strong positive cluster of sucrose,
283 galactinol, and raffinose in *stvinv* plants (Fig. S3A), reflecting a coordinated sugar-
284 based response. WT plants, in contrast, showed more diffuse correlation networks
285 involving amino acids and secondary metabolites (Fig. S3B), consistent with a broader
286 metabolic adjustment under stress. Sparse PLS-DA analysis WT plants were
287 characterized by early-stage peaks in homoserine and dihydrosphingosine, suggesting
288 a transient stress-reactive response (Fig. 5C). In *stvinv* lines, galactinol, raffinose, and
289 glucose-6-phosphate levels were higher than WT the drought and recovery phases (Fig.

290 5D). By reducing reliance on energy-intensive pathways and enhancing osmoprotective
291 sugar accumulation and carbon recycling, the *stvinv* plants minimized stress perception
292 and maintained physiological homeostasis more effectively than their WT counterparts.
293 Together, these findings indicate that *stvinv* plants adopt a focused, sugar-centered
294 metabolic strategy to mitigate drought stress.

295 **Drought tolerance of *stvinv* is associated with elevated RFO metabolism in leaves.**

296 Our previous work demonstrated that *stvinv* plants showed increased expression of RFO
297 biosynthetic genes followed by higher levels of RFOs in potato tuber parenchyma in
298 response to cold stress [29]. Given this finding, we hypothesized that the enhanced
299 drought tolerance observed in *stvinv* plants might similarly involve RFO metabolism.
300 Metabolomic profiling revealed that all genotypes exhibited a general trend of reduced
301 glucose-6-phosphate and sucrose levels, alongside increased galactose, galactinol, and
302 raffinose levels during drought and recovery phases (Fig. 6). However, *stvinv* plants
303 showed, during drought and recovery from drought, higher levels of sucrose, galactinol
304 and raffinose, and lower levels of myo-inositol compared to WT plants (Fig. 6). These
305 results suggest that *stvinv* plants may metabolize RFO more effectively, contributing to
306 their ability to maintain physiological and biochemical homeostasis under drought
307 conditions.

308 **Drought tolerance of *stvinv* plants is associated with reduced ABA and its**

309 **catabolites.** To assess the hormonal response associated with early drought adaptation,
310 ABA and its catabolic derivatives phaseic acid (PA) and dehydrophaseic acid (DPA)
311 were quantified using LC-MS. Samples were collected from one-month-old plants at
312 baseline (prior to drought; irrigation phase) and after 7 days of drought exposure. As
313 expected, all genotypes exhibited elevated ABA levels in response to drought.

314 However, *stvinv-7* and *stvinv-8* accumulated significantly lower levels of ABA, PA,
315 and DPA during drought, compared to WT plants (Fig. 7). These findings suggest that
316 drought tolerance in *stvinv* plants may be facilitated by controlled ABA response,
317 complimented by induction of higher RFO levels.

318

319 **Discussion**

320 **Enhanced drought resilience and resource efficiency in *stvinv* plants**

321 Drought is a major constraint on potato production, and its impact is expected to worsen
322 with climate change [45]. It has been shown to disrupt carbon partitioning, leading to
323 sugar accumulation in sink leaves and reduced tuber yield and number [45, 46]. The
324 *stvinv* plants exhibited significantly enhanced drought resistance by maintaining
325 consistently higher stomatal conductance, transpiration rates, and photosynthetic
326 efficiency compared to WT plants during both drought and recovery phases (Figs. 1
327 and 2). Typically, drought stress induces stomatal closure to reduce water loss, but this
328 response comes at the cost of CO₂ assimilation and metabolic activity [59-61]. In
329 contrast, *stvinv* plants maintained open stomata under drought, supporting an
330 unconventional (risk taking) strategy that enables continuous carbon assimilation and
331 sustained energy production despite water limitations. A key advantage of this strategy
332 lies in the knockout plants' ability to balance elevated transpiration with efficient
333 internal water regulation and minimal tissue damage as revealed by its fast recovery.
334 Despite higher transpiration rate, *stvinv* plants displayed superior AWUE, likely
335 facilitated by their enhanced osmotic adjustment and anticipatory metabolic responses
336 (Fig. 3). Metabolomic profiling of *stvinv* and WT plants revealed significant
337 accumulation of osmoprotective sugars, particularly galactinol and raffinose (Fig. 5),

338 which help maintain cellular water balance and preserve turgor under drought [19, 62].
339 In addition to supporting photosynthesis, elevated transpiration rate in *stvinv* plants
340 increases evaporative cooling, effectively lowering leaf temperature [63], which in turn,
341 curtail heat-induced ROS production [60, 64]. These protective effects are further
342 reinforced by the ROS-scavenging function of RFOs [19, 65, 66]. We previously
343 showed that, under cold stress, RFO accumulation in *stvinv* plants was linked to
344 decreased ROS levels [67], suggesting the presence of a conserved sugar-mediated
345 mechanism for mitigating oxidative stress that may also operate under drought
346 conditions.

347 Recent evidence also indicates that osmolyte accumulation, such as elevated RFOs,
348 may positively influence mesophyll conductance (g_m), the diffusion of CO₂ from
349 intercellular spaces to chloroplasts. Enhanced g_m under drought conditions has been
350 associated with improved photosynthetic performance and water-use efficiency due to
351 better membrane stability and reduced oxidative stress [19, 60, 68-70]. Although g_m
352 was not directly measured in our study, the observed physiological and metabolic traits
353 of *stvinv* plants, including sustained gas exchange, enhanced osmolyte accumulation,
354 and stable photosynthetic capacity (Figs 1-3) are consistent with a scenario in which
355 improved g_m contributes substantially to their drought resilience.

356 *stvinv* plants maintain both elevated transpiration and biomass accumulation (Figs 1-4),
357 demonstrating resilience to drought stress. Importantly, this increase in biomass
358 accumulation, particularly in shoot tissue, is not accompanied by a reduction in tuber
359 productivity (Fig. 4). While total tuber weight did not significantly differ between
360 genotypes, *stvinv-7* produced a slightly higher number of tubers under drought (Fig. 4).
361 This finding suggests that the enhanced shoot vigor in *stvinv* plants, reinforcing their

362 agronomic potential in drought-prone environments allowing the plant to survive longer
363 and potentially produce higher yield.

364 The rapid recovery of *stvinv* plants following rehydration (Fig. 2) suggests an enhanced
365 capacity to maintain or quickly restore metabolic function. Such resilience could be
366 mediated by sustained sugar signaling and a reduced internal perception of stress,
367 potentially involving transcriptional or epigenetic memory mechanisms [71, 72].
368 Indeed, the muted accumulation of drought-induced stress metabolites such as proline,
369 homoserine, and shikimic acid in *stvinv* plants (Figs 5 and S2) supports the hypothesis
370 that these plants inherently perceive lower stress levels under drought compared to WT
371 plants.

372 Collectively, these findings indicate that *stvinv* plants adopt a productive drought
373 strategy, integrating elevated transpiration, osmolyte-based stress buffering,
374 evaporative cooling, and potentially primed recovery mechanisms to sustain growth
375 and yield.

376 **Resilience supported by metabolic shifts and RFO pathway induction**

377 The drought resilience of *stvinv* plants is further supported by extensive metabolic
378 reprogramming. Elevated levels of citric acid and enhanced activation of glyoxylate
379 and dicarboxylate metabolism pathways indicate improved carbon recycling and energy
380 conservation under stress [73]. These changes likely provide sufficient ATP to sustain
381 basal metabolism and enable rapid recovery after rehydration.

382 A central aspect of this metabolic shift is the robust activation of the RFO biosynthetic
383 pathway. Metabolomic profiling revealed elevated galactinol and raffinose levels in
384 *stvinv* plants under drought, along with reduced myo-inositol content, indicating a
385 preferential flux toward RFO production. These sugars are known osmoprotectants that

386 stabilize membranes and proteins, helping maintain turgor and mitigate dehydration
387 effects [74-76].

388 In addition to osmoprotection, galactinol and raffinose act as direct ROS scavengers,
389 contributing to oxidative stress reduction [65, 77-79]. Their accumulation likely
390 reduces reliance on energy-intensive antioxidant systems. This is consistent with the
391 reduced accumulation of stress markers like proline, homoserine, and shikimic acid in
392 *stvinv* plants. Our previous work showed that under cold stress, elevated RFO levels in
393 *stvinv* plants were associated with reduced ROS accumulation [67], suggesting that
394 similar sugar-based mechanisms operate under drought.

395 The enhanced expression of *GolS3* and *MIP2*, key genes in galactinol biosynthesis and
396 sugar transport, further supports the notion that *stvinv* plants prioritize RFO metabolism
397 under stress. High sucrose levels detected in *stvinv* plants may serve not only as a carbon
398 source for RFO synthesis but also as part of an alternative metabolic route, as proposed
399 in our previous work [67]. Under cold stress, *stvinv* plants shifted toward RFO-
400 producing pathway in the absence of vacuolar invertase, a mechanism likely conserved
401 under drought. Recent findings also suggest that ABA signaling, via ABF-type
402 transcription factors such as CsABF8, can activate RFO biosynthetic genes under
403 drought [80]. The ability of *stvinv* plants to maintain high RFO levels despite low ABA
404 concentrations implies the existence of ABA-independent or sugar-mediated regulatory
405 routes, reinforcing the functional redundancy and plasticity of RFO-inducing
406 mechanisms under stress.

407 As a central soluble carbohydrate, sucrose may support drought resilience by serving
408 as a rapid energy source, stabilizing osmotic potential, and promoting turgor
409 maintenance [81]. Additionally, sucrose acts as a precursor for RFO biosynthesis and a

410 signaling molecule that can attenuate stress-induced ABA responses or modulate gene
411 expression through ABA-independent pathways [77, 82-86].

412 Although direct ROS scavenging by sucrose is less established than for RFOs, it may
413 contribute modestly to redox buffering via sugar-regulated ROS genes and interactions
414 with other antioxidants [66, 81, 86-88]. Its primary impact, however, likely reflects
415 energetic efficiency and signaling functions. Together, these roles support the view that
416 elevated sucrose in *stvinv* plants enhances metabolic flexibility and hormonal balance
417 under drought, while promoting the biosynthesis of protective oligosaccharides.

418 This sugar-centric metabolic strategy may also reflect a broader shift from nitrogen-
419 intensive stress responses (e.g., proline accumulation) to carbon-based protective
420 mechanisms (Figs. 5 and 6). This shift could reduce the metabolic cost of stress
421 adaptation, preserving nitrogen for growth-related functions [89-91]. This is further
422 supported by the consistently lower levels of classical stress markers, indicating that
423 *stvinv* plants likely perceive and experience less physiological stress compared to WT
424 under drought conditions.

425 Together, the coordinated accumulation of protective sugars, reduced ROS burden,
426 energy-saving metabolic shifts, and lower stress metabolite levels define a sugar-
427 centered, anticipatory strategy that buffers stress perception and sustains physiological
428 function under drought. This profile resembles anisohydric “risk-taking” behavior—
429 maintaining stomatal opening and productivity under moderate drought—and relies on
430 tightly linked hormonal control, in which attenuated ABA signaling and sugar-mediated
431 modulation jointly contribute to drought resilience [92].

432 **Attenuated ABA signaling and sugar-mediated hormonal modulation contribute**
433 **to drought resilience**

434 ABA, which is synthesized mainly in the leaves [93], is a central regulator of plant
435 drought responses, typically inducing stomatal closure and restricting growth to
436 conserve water [94-96]. However, *stvinv* plants accumulated significantly lower levels
437 of ABA and its catabolites (PA and DPA) under drought compared to WT plants (Fig.
438 7). This attenuated ABA response likely reduces the growth penalties commonly
439 associated with prolonged ABA signaling [97, 98], enabling *stvinv* plants to maintain
440 higher stomatal conductance and thus sustain gas exchange, carbon assimilation, and
441 growth even under limited water availability.

442 A probable mechanism behind this hormonal modulation involves sugar signaling,
443 particularly via hexokinase (HXK), which functions both as a glycolytic enzyme and a
444 glucose sensor modulating ABA responses [82, 99]. Reduced vacuolar invertase
445 activity in *stvinv* plants could limit cytosolic glucose availability, dampening HXK-
446 mediated ABA signaling and facilitating prolonged stomatal opening, thus maintaining
447 physiological activity during drought. This risk-taking strategy could potentially expose
448 plants to desiccation, xylem embolism, or other hydraulic damages. However, the rapid
449 post-drought recovery of *stvinv* plants suggests that they did not incur significant costs
450 for sustaining higher activity under water limitation. It is possible that this resilience is
451 linked to their distinct metabolic adjustments, which mitigate stress damage and support
452 continued function under adverse conditions. The metabolic profile of *stvinv* plants
453 further supports this model. Unlike WT plants, which accumulate stress metabolites
454 such as proline, homoserine, and shikimic acid, *stvinv* plants exhibited reduced levels
455 of these compounds, highlighting their inherently lower stress perception and reduced
456 internal stress signaling [100]. Instead, their metabolic strategy favored accumulating
457 raffinose and galactinol, which provide robust osmoprotection and ROS detoxification,
458 contributing to their drought resilience [36, 74, 79, 101]. Moreover, our previous

459 research under cold stress demonstrated a clear correlation between enhanced RFO
460 accumulation and reduced ROS levels in *stvinv* plants [29]. Given the comparable
461 metabolic response observed under drought, it is plausible that sugar-mediated
462 hormonal crosstalk, potentially involving HXK, ABA, and RFO metabolism,
463 constitutes a conserved regulatory module that buffers stress perception, supports
464 physiological homeostasis, and improves resilience across various abiotic stresses.

465 Recent studies have further highlighted the role of sugars in modulating ABA
466 sensitivity and response through sugar-responsive transcription factors and signaling
467 pathways, reinforcing the importance of sugar-ABA crosstalk in environmental stress
468 tolerance [102-104]. Such integration likely contributes significantly to the *stvinv*
469 plants' efficient stress response, energy conservation, and sustained growth.

470 This shift from reactive to buffered responses may enable *stvinv* plants to avoid costly
471 metabolic penalties associated with conventional stress responses, thus defining a novel
472 and energy-efficient adaptation strategy under drought conditions.

473 **Non-structural stomatal regulation complements metabolic adaptation**

474 Despite their elevated stomatal conductance, *stvinv* plants did not differ from WT in
475 stomatal density or aperture size. This observation highlights that drought resilience in
476 *stvinv* plants does not result from structural leaf adaptations but rather from functional
477 plasticity in stomatal regulation. Such functional plasticity, modulated by sugar and
478 ABA signaling pathways, allows dynamic optimization of water loss and carbon
479 assimilation under varying environmental conditions (Fig. 8) [59, 105].

480 Together, these coordinated physiological and metabolic adjustments allow *stvinv*
481 plants to sustain growth and photosynthesis during water deficit. Their drought
482 response strategy represents a transition from passive resistance to active stress

483 management, highlighting their potential as valuable models for engineering stress
484 resilience in crop species.

485

486 **Methods**

487 **Plant growth conditions and drought stress treatment**

488 *Solanum tuberosum* cv. Désirée plants were propagated in tissue culture for 3 weeks
489 and transferred to small pots (4.5 × 8.5 cm) containing standard potting mix (Pelemix
490 Green) for an additional 4 weeks. Seedlings were maintained in a controlled growth
491 chamber under a 16 h light/8 h dark photoperiod at 23 °C, with ~200 μmol m⁻² s⁻¹
492 photosynthetically active radiation provided by LED illumination.

493 Plants were irrigated twice daily until stress induction. Drought stress was imposed by
494 withholding irrigation for 15-18 consecutive days, followed by rewatering to monitor
495 recovery responses over a 12-day period. Drought response was visually evaluated
496 using a phenotypic scale ranging from 1 to 10, where a score of 10 represented a high-
497 vigor plant and a score of 1 indicated severe wilting. Physiological and biochemical
498 measurements were conducted before, during, and after the drought cycle to assess plant
499 performance and stress resilience. Each genotype was represented by a minimum of 8
500 biological replicates (8–12 plants per treatment), ensuring robust statistical evaluation
501 of drought responses.

502 **Physiological measurements under drought stress**

503 Leaf stomatal conductance and chlorophyll fluorescence were measured using the LI-
504 600 and LI-600N Porometer/Fluorometer (LI-COR Biosciences), which
505 simultaneously records gas exchange and photosynthetic efficiency from the same leaf
506 area. Measurements were performed daily on fully expanded mature leaves from the
507 second node below the apical bud, at a fixed time point, one hour after lights-on. This

508 time was chosen to allow for stabilization of photosynthetic activity following the dark-
509 to-light transition, while minimizing diurnal variability.

510 Chlorophyll content was assessed non-destructively using a SPAD-502 Plus
511 Chlorophyll Meter (Konica Minolta, Japan), which estimates relative chlorophyll
512 concentration based on leaf light transmittance. Measurements were performed on the
513 same leaves used for gas exchange analyses, with three readings per leaf averaged to
514 yield a single value per plant. At least 10 biological replicates per genotype were
515 analyzed across all time points.

516 **Whole plant water relations phenotyping using a lysimetric array (Plantarray)**

517 Physiological phenotyping, including whole-plant measurement of transpiration
518 dynamics, canopy stomatal conductance, and water-use efficiency (WUE), was
519 performed using the Plantarray 3.0 high-throughput functional phenotyping platform
520 (Plant-DiTech, Israel), following established protocols [106]. Potato tuber sprouts were
521 excised at the nodal region and planted in a soil mixture consisting of polystyrene:
522 vermiculite: peat moss in a 3:2:1 ratio (v/v). Seedlings were grown in a greenhouse
523 under natural day length and ambient Mediterranean winter conditions; temperatures
524 ranging between 15°C and 32°C, relative humidity between 25% and 40%, and a
525 photoperiod of ~11 h light/13 h dark, with all environmental parameters (temperature,
526 humidity, PAR, VPD) continuously monitored, see supplementary Fig. S4 [106, 107].
527 Average PAR during daytime was ~600–1200 $\mu\text{mol m}^{-2} \text{s}^{-1}$. After one month, plants
528 were transferred to the ICORE Center for Functional Phenotyping greenhouse for an
529 additional month of acclimation under daily irrigation. Subsequently, two-month-old
530 plants were transferred to the lysimetric array and grown for 34 days (3 March–4 April
531 2022) in 4-L pots filled with sand 20/30 (Negev Minerals) under natural sunlight and

532 moderately controlled temperature conditions, simulating near-field environments
533 [108, 109]. To prevent soil evaporation, pots were covered with a plastic film.
534 The experiment was conducted in a randomized block design. The experiment followed
535 a randomized design, with 8–14 biological replicates per genotype in the drought
536 treatment and 3–4 well-watered controls per genotype maintained under full irrigation.
537 Soil volumetric water content (VWC) was continuously monitored via 5TE (Meter,
538 USA) sensors placed in each pot, while environmental variables were recorded to
539 compute vapor pressure deficit (VPD: 0.7–4.0 kPa) (Supplementary Fig. S4). Whole-
540 plant transpiration-rate was measured gravimetrically at 3-minute intervals by
541 analyzing changes in pot weight using high-resolution load cells, enabling continuous
542 monitoring of water fluxes in the soil-plant-atmosphere continuum [108]. A three-phase
543 irrigation regime was applied: (i) well-watered pretreatment (days 1–12); (ii) drought
544 induction (days 13–27), during which irrigation was reduced daily to 80% of each
545 plant’s previous-day transpiration, mimicking progressive soil water depletion as
546 occurs in field conditions [110]; and (iii) full re-irrigation recovery (days 28–34). The
547 Plantarray platform includes a feedback-controlled irrigation system that ensures
548 uniform drought exposure across genotypes by tailoring water delivery to each plant’s
549 individual transpiration rate [106]. Processed data were analyzed via the SPAC
550 Analytics web tool, which supports both real-time visualization and statistical analysis
551 of multiple parameters, including transpiration rate, stomatal conductance, growth rate,
552 and WUE. WUE was calculated daily as the ratio of modeled daily biomass gain to
553 daily transpiration, as implemented in SPAC Analytics. Agronomic water-use
554 efficiency (AWUE) was computed per plant as final total dry biomass divided by
555 cumulative transpiration over the full experimental period: $AWUE = (DW_{shoot} +$
556 $DW_{tuber} + DW_{root}) / \int Transpiration dt$, where dry biomass was determined at

557 harvest after oven-drying, and cumulative transpiration ($L \text{ plant}^{-1}$) was obtained by
558 time-integrating the load-cell mass balance with irrigation inputs and drainage
559 subtracted; units $g \text{ L}^{-1}$.

560 **Tissue sampling**

561 For metabolomic analysis, fully expanded young leaves were sampled from the third
562 node below the apical bud at six distinct time points: T0 (baseline, following 10 days
563 of full irrigation), T1 and T2 (mild drought, after 7 and 9 days without irrigation,
564 respectively), T3 and T4 (progressive drought, after 12 and 14 days without irrigation),
565 and T5 (recovery, one day after rewatering). For ABA quantification, leaf samples were
566 collected at two time points: baseline (during the irrigation phase) and at the middle of
567 the drought phase (day 7). All samples were collected at midday from well-expanded
568 leaves to minimize diurnal variation, immediately frozen in liquid nitrogen, and stored
569 at $-80 \text{ }^{\circ}\text{C}$ until further analysis.

570 **Quantitative analysis of ABA metabolites**

571 Endogenous levels of ABA and its metabolites were assessed as previously described:
572 sample purification and chromatographic separation was performed according to
573 Danieli et al. [111] and settings for the MS detection were according to Vrobel et al.
574 [112]. Briefly, 3 mg of homogenized lyophilized leaves were extracted with 1 ml of
575 50% aqueous acetonitrile containing a mixture of internal standards (4 pmol of D6-
576 ABA, D3-PA and D3-DPA per sample) on ice-cold ultrasonic bath for 30 min. After
577 centrifugation (20 000 g, 10 min, 4°C) the supernatant was loaded onto an Oasis HLB
578 column (1 ml cartridge, 30 mg sorbent, Waters, USA) equilibrated with 1 ml methanol,
579 1 ml water and lastly by 1 ml 50 % acetonitrile. Flow-through fraction was collected
580 and pooled with elution solvent, 1 ml of 30% acetonitrile. Pooled fractions were
581 evaporated *in vacuo*. Prior to analysis, samples were resuspended in 40 μL of mobile

582 phase and analyzed. Analyses were performed using a Nexera X2 modular liquid
583 chromatograph coupled to an MS 8050 triple quadrupole mass spectrometer
584 (Shimadzu) via an electrospray interface. Chromatographic separation was performed
585 using Waters analytical column CSH™ C18, 2.1 mm × 150 mm, 1.7 μm. Aqueous
586 solvent A consisted of 15 mM formic acid adjusted to pH 3.0 with ammonium
587 hydroxide. Solvent B was acetonitrile. Separation was achieved by gradient elution at
588 a flow rate of 0.4 mL/min at 40°C: 0–1 min 20% B; 1–11 min 80% B in a linear gradient,
589 followed by washing and equilibration to initial conditions for a further 7 min. Three
590 MRM transitions were monitored for each analyte (ABA, PA, DPA, ABA-GE and
591 internal standards) to ensure correct identification. Raw data were processed using
592 Shimadzu software LabSolutions ver. 5.97 SP1.

593 **Extraction of primary metabolites**

594 Metabolite analysis by GC-MS was carried out by a method modified from that
595 described previously (Roessner et al., 2001) extracted in 1 ml prechilled
596 methanol:chloroform:water extraction solution (2.5:1:1 v/v) with 380 μl of Standards
597 (1 mg/ml ribitol in water) subsequently added as a internal standard. The mixture was
598 sonication for 10 min, shaking for 10 min at 25°C. After centrifugation at 14000 RPM,
599 300 μL of water and chloroform was added to the supernatant. Following vortexing and
600 centrifugation the methanol-water phase was taken and kept at –80°C until use.

601 **Derivatization and analysis of primary metabolites in GC-MS**

602 200 μL of methanol-water phase reduced to dryness in vacuum. Residues were
603 redissolved and derivatized for 120 min at 37°C in 40 μL of 20 mg/mL methoxyamine
604 hydrochloride in pyridine) followed by a 30-min treatment with 70 μL N-methyl-N-
605 (trimethylsilyl)trifluoroacetamide at 37°C. 7 microliters of a retention time standard
606 mixture (0.029% v/v n-dodecane, n-pentadecane, n-nonadecane, n-docosane, n-

607 octacosane, n-dotracontane, and n-hexatriacontane dissolved in pyridine) was added
608 prior to trimethylsilylation. The first run was done by injecting 1 μ L to analyse
609 melibiose and second run was performed with 0.2 μ L to analyse galactose. Both runs
610 were done in splitless mode. The GC-MS system consisted of a 7693 autosampler, a
611 7890B GC, and a 5977B single quadrupole mass spectrometer (Agilent ltd). The mass
612 spectrometer was tuned according to the manufacturer's recommendations using tris-
613 (perfluorobutyl)-amine (CF43). GC was performed on a 30 m VF-5ms column with
614 0.25 mm i.d. and 0.25 μ m film thickness +10 m EZ-Guard (Agilent). (Split/splitless liner
615 with Wool, Restek, USA). Gradient of Injection temperature (PTV) was from 70°C to
616 300°C in 14.5°C/sec, the Transfer line was 350°C, and the ion source adjusted to 250°C.
617 Gain factor 15. The carrier gas used was helium set at a constant flow rate of 1 ml/ min.
618 The temperature program was 1 min isothermal heating at 70°C, followed by a 1°C/min
619 oven temperature ramp to 76°C, followed by a 6°C/min oven temperature ramp to
620 340°C, and a final 5 min heating at 340°C. Mass spectra were recorded at 1.6 scans per
621 second with a mass-to-charge ratio 70 to 550 scanning range. Post-column Back-
622 flushing was used during the post-run time in every injection to keep detector clean,
623 column flow was reversed for few minutes to remove high-boiling components to inlet
624 split vent. JetClean procedure was used after 1 μ L set (15 injections) to keep the ion
625 source clean, based on reductive hydrogen cleaning principle. Spectral searching in the
626 Masshunter software (Qualitative and Unknown analyses) against RI libraries
627 downloadable from the Max-Planck Institute for Plant Physiology in Golm,
628 (<http://gmd.mpimp-golm.mpg.de/>) the result normalized by the internal standard ribitol
629 and the average of the pools, and finally by log transformation.

630 **Metabolomic data analysis**

631 Raw metabolite abundance data were preprocessed, normalized, and statistically
632 analyzed using the web-based platform MetaboAnalyst 5.0
633 (<https://www.metaboanalyst.ca>)[113]. Data normalization included log transformation
634 and auto-scaling to facilitate downstream multivariate analyses. Principal component
635 analysis (PCA) and partial least squares-discriminant analysis (PLS-DA) were
636 performed to assess clustering and group separation. Differential metabolites were
637 identified using univariate statistics (Student's *t*-test, FDR-adjusted $P < 0.05$) and
638 visualized using volcano plots and heatmaps. Enrichment and pathway analyses were
639 conducted using the *Arabidopsis thaliana* reference pathway library, based on KEGG
640 and SMPDB

641 **Stomatal density and aperture**

642 Stomatal traits were quantified using a rapid dental-resin imprinting method following
643 Geisler [114, 115]. Fully expanded leaves that had reached final size were sampled from
644 the third node below the apical bud, from well-watered plants grown under controlled
645 long-day conditions (16 h light: 8 h dark). Sampling was conducted at mid-morning,
646 approximately 1 h after lights-on (09:30–10:30 local time), to minimize diurnal
647 variation in stomatal aperture. Stomata and impressions of the abaxial (lower) and
648 adaxial (upper) epidermis were taken by gently applying a thin layer of clear dental
649 resin (Zhermack Elite HD). After drying (~10–15 min), the resin was covered with nail
650 polish and covered with film. The film was peeled off and mounted onto microscope
651 slides. This method preserves stomatal morphology and distribution with high fidelity,
652 allowing for accurate microscopic analysis.

653 Imprints were visualized using bright-field light microscopy at $\times 200$ – $\times 400$
654 magnification. Stomatal density (number of stomata per mm^2) was quantified by
655 counting stomata within defined calibrated areas. Stomatal aperture width, defined as

656 the distance between the inner edges of the guard cells, was measured using an eyepiece
657 micrometer and validated by ImageJ, a digital image analysis software [116].
658 Multiple fields per sample (typically 3–5) were analyzed to account for spatial
659 variability across the leaf surface, and at least three biological replicates per genotype
660 were used. This approach enabled us to detect subtle differences in stomatal
661 morphology and behavior under drought and control conditions.

662 **Harvest and biomass measurements**

663 At the conclusion of the experiment, whole plants were harvested and separated into
664 three major components: aboveground green tissues (including fully expanded leaves
665 and stems), roots, and tubers. Each plant part was immediately weighed to determine
666 fresh biomass. Leaf and stem tissues were then air-dried at room temperature for 7 days,
667 followed by oven-drying at 60 °C until constant weight. The resulting dry weight of
668 aboveground green tissues was recorded for subsequent analysis.

669 **Data availability**

670 All data supporting the findings of this study are available within the article and its
671 supplementary information files.

672

673 **References**

- 674 1. Ritonga, F.N. and S. Chen, *Physiological and molecular mechanism involved*
675 *in cold stress tolerance in plants*. *Plants*, 2020. **9**: 560.
- 676 2. Miller, G.,N. Suzuki,S. Ciftci-Yilmaz, and R. Mittler, *Reactive oxygen species*
677 *homeostasis and signalling during drought and salinity stresses*. *Plant, Cell &*
678 *Environment*, 2010. **33**: 453-467.

- 679 3. Zhang, J.,X.-M. Li,H.-X. Lin, and K. Chong, *Crop improvement through*
680 *temperature resilience*. Annual Review of Plant Biology, 2019. **70**: 753-780.
- 681 4. Yamaguchi-Shinozaki, K. and K. Shinozaki, *Organization of cis-acting*
682 *regulatory elements in osmotic-and cold-stress-responsive promoters*. Trends
683 in Plant Science, 2005. **10**: 88-94.
- 684 5. Hasanuzzaman, M.,M. Bhuyan,K. Parvin,T.F. Bhuiyan,T.I. Anee,K. Nahar,M.
685 Hossen,F. Zulfiqar,M. Alam, and M. Fujita, *Regulation of ROS metabolism in*
686 *plants under environmental stress: A review of recent experimental evidence*.
687 International Journal of Molecular Sciences, 2020. **21**: 8695.
- 688 6. Das, K. and A. Roychoudhury, *Reactive oxygen species (ROS) and response of*
689 *antioxidants as ROS-scavengers during environmental stress in plants*.
690 Frontiers in environmental science, 2014. **2**: 53.
- 691 7. Gill, S.S. and N. Tuteja, *Reactive oxygen species and antioxidant machinery in*
692 *abiotic stress tolerance in crop plants*. Plant Physiology and Biochemistry,
693 2010. **48**: 909-930.
- 694 8. Suprasanna, P.,G. Nikalje, and A. Rai, *Osmolyte accumulation and implications*
695 *in plant abiotic stress tolerance*, in *Osmolytes and Plants Acclimation to*
696 *Changing Environment: Emerging Omics Technologies*. 2016, Springer. p. 1-
697 12.
- 698 9. Khan, M.S.,D. Ahmad, and M.A. Khan, *Utilization of genes encoding*
699 *osmoprotectants in transgenic plants for enhanced abiotic stress tolerance*.
700 Electronic Journal of Biotechnology, 2015. **18**: 257-266.
- 701 10. Qi, X.,Z. Wu,J. Li,X. Mo,S. Wu,J. Chu, and P. Wu, *AtCYT-INV1, a neutral*
702 *invertase, is involved in osmotic stress-induced inhibition on lateral root growth*
703 *in Arabidopsis*. Plant Molecular Biology, 2007. **64**: 575-587.

- 704 11. Liu, H.,C. Yu,H. Li,B. Ouyang,T. Wang,J. Zhang,X. Wang, and Z. Ye,
705 *Overexpression of ShDHN, a dehydrin gene from Solanum habrochaites*
706 *enhances tolerance to multiple abiotic stresses in tomato*. Plant Science, 2015.
707 **231**: 198-211.
- 708 12. Wind, J.,S. Smeekens, and J. Hanson, *Sucrose: metabolite and signaling*
709 *molecule*. Phytochemistry, 2010. **71**: 1610-1614.
- 710 13. Keunen, E.,D. Peshev,J. Vangronsveld,W. Van Den Ende, and A. Cuypers,
711 *Plant sugars are crucial players in the oxidative challenge during abiotic stress:*
712 *extending the traditional concept*. Plant, Cell & Environment, 2013. **36**: 1242-
713 1255.
- 714 14. Andreev, I., *Role of the vacuole in the redox homeostasis of plant cells*. Russian
715 Journal of Plant Physiology, 2012. **59**: 611-617.
- 716 15. Valluru, R. and W. Van den Ende, *Plant fructans in stress environments:*
717 *emerging concepts and future prospects*. Journal of Experimental Botany, 2008.
718 **59**: 2905-2916.
- 719 16. Van den Ende, W. and R. Valluru, *Sucrose, sucrosyl oligosaccharides, and*
720 *oxidative stress: scavenging and salvaging?* Journal of Experimental Botany,
721 2009. **60**: 9-18.
- 722 17. Smeekens, S.,J. Ma,J. Hanson, and F. Rolland, *Sugar signals and molecular*
723 *networks controlling plant growth*. Current Opinion in Plant Biology, 2010. **13**:
724 273-278.
- 725 18. Tarkowski, Ł.P. and W. Van den Ende, *Cold tolerance triggered by soluble*
726 *sugars: a multifaceted countermeasure*. Frontiers in plant science, 2015. **6**: 203.

- 727 19. Nishizawa, A.,Y. Yabuta, and S. Shigeoka, *Galactinol and raffinose constitute*
728 *a novel function to protect plants from oxidative damage*. Plant Physiology,
729 2008. **147**: 1251-1263.
- 730 20. Wang, K.,X. Shao,Y. Gong,Y. Zhu,H. Wang,X. Zhang,D. Yu,F. Yu,Z. Qiu, and
731 H. Lu, *The metabolism of soluble carbohydrates related to chilling injury in*
732 *peach fruit exposed to cold stress*. Postharvest biology and technology, 2013.
733 **86**: 53-61.
- 734 21. Wang, X.,Y. Chen,S. Jiang,F. Xu,H. Wang,Y. Wei, and X. Shao, *PpINH1, an*
735 *invertase inhibitor, interacts with vacuolar invertase PpVIN2 in regulating the*
736 *chilling tolerance of peach fruit*. Horticulture research, 2020. **7**: 1-14.
- 737 22. Morsy, M.R.,L. Jouve,J.-F. Hausman,L. Hoffmann, and J.M. Stewart,
738 *Alteration of oxidative and carbohydrate metabolism under abiotic stress in two*
739 *rice (Oryza sativa L.) genotypes contrasting in chilling tolerance*. Journal of
740 Plant Physiology, 2007. **164**: 157-167.
- 741 23. Gu, H.,M. Lu,Z. Zhang,J. Xu,W. Cao, and M. Miao, *Metabolic process of*
742 *raffinose family oligosaccharides during cold stress and recovery in cucumber*
743 *leaves*. Journal of Plant Physiology, 2018. **224**: 112-120.
- 744 24. Salvi, P.,N.U. Kamble, and M. Majee, *Stress-inducible galactinol synthase of*
745 *chickpea (CaGols) is implicated in heat and oxidative stress tolerance through*
746 *reducing stress-induced excessive reactive oxygen species accumulation*. Plant
747 and cell physiology, 2018. **59**: 155-166.
- 748 25. Hinch, D.K.,E. Zuther, and A.G. Heyer, *The preservation of liposomes by*
749 *raffinose family oligosaccharides during drying is mediated by effects on fusion*
750 *and lipid phase transitions*. Biochimica et Biophysica Acta (BBA)-
751 Biomembranes, 2003. **1612**: 172-177.

- 752 26. Ma, S.,J. Lv,X. Li,T. Ji,Z. Zhang, and L. Gao, *Galactinol synthase gene 4*
753 *(CsGolS4) increases cold and drought tolerance in Cucumis sativus L. by*
754 *inducing RFO accumulation and ROS scavenging*. Environmental and
755 experimental botany, 2021. **185**: 104406.
- 756 27. Salvi, P.,N.U. Kamble, and M. Majee, *Ectopic over-expression of ABA-*
757 *responsive Chickpea galactinol synthase (CaGolS) gene results in improved*
758 *tolerance to dehydration stress by modulating ROS scavenging*. Environmental
759 and experimental botany, 2020. **171**: 103957.
- 760 28. Klotke, J.,J. Kopka,N. Gatzke, and A. Heyer, *Impact of soluble sugar*
761 *concentrations on the acquisition of freezing tolerance in accessions of*
762 *Arabidopsis thaliana with contrasting cold adaptation—evidence for a role of*
763 *raffinose in cold acclimation*. Plant, Cell & Environment, 2004. **27**: 1395-1404.
- 764 29. Teper-Bamnlker, P.,M. Roitman,O. Katar,N. Peleg,K. Aruchamy,S. Suher,A.
765 Doron-Faigenboim,D. Leibman,A. Omid, and E. Belausov, *An alternative*
766 *pathway to plant cold tolerance in the absence of vacuolar invertase activity*.
767 The Plant Journal, 2023. **113**: 327-341.
- 768 30. Gangl, R. and R. Tenhaken, *Raffinose family oligosaccharides act as galactose*
769 *stores in seeds and are required for rapid germination of Arabidopsis in the*
770 *dark*. Frontiers in plant science, 2016. **7**: 1115.
- 771 31. Saito, M. and M. Yoshida, *Expression analysis of the gene family associated*
772 *with raffinose accumulation in rice seedlings under cold stress*. Journal of Plant
773 Physiology, 2011. **168**: 2268-2271.
- 774 32. Karner, U.,T. Peterbauer,V. Raboy,D.A. Jones,C.L. Hedley, and A. Richter,
775 *myo-Inositol and sucrose concentrations affect the accumulation of raffinose*

- 776 *family oligosaccharides in seeds*. Journal of Experimental Botany, 2004. **55**:
777 1981-1987.
- 778 33. Bernal-Lugo, I. and A. Leopold, *Seed stability during storage: Raffinose*
779 *content and seed glassy state I*. Seed Science Research, 1995. **5**: 75-80.
- 780 34. Salvi, P.,S.C. Saxena,B.P. Petla,N.U. Kamble,H. Kaur,P. Verma,V. Rao,S.
781 Ghosh, and M. Majee, *Differentially expressed galactinol synthase (s) in*
782 *chickpea are implicated in seed vigor and longevity by limiting the age induced*
783 *ROS accumulation*. Scientific Reports, 2016. **6**: 35088.
- 784 35. Bolouri-Moghaddam, M.R.,K. Le Roy,L. Xiang,F. Rolland, and W. Van den
785 Ende, *Sugar signalling and antioxidant network connections in plant cells*. The
786 FEBS Journal, 2010. **277**: 2022-2037.
- 787 36. ElSayed, A.I.,M.S. Rafudeen, and D. Golldack, *Physiological aspects of*
788 *raffinose family oligosaccharides in plants: protection against abiotic stress*.
789 Plant Biology, 2014. **16**: 1-8.
- 790 37. Cruz de Carvalho, M.H., *Drought stress and reactive oxygen species:*
791 *production, scavenging and signaling*. Plant Signaling & Behavior, 2008. **3**:
792 156-165.
- 793 38. Fàbregas, N. and A.R. Fernie, *The metabolic response to drought*. Journal of
794 Experimental Botany, 2019. **70**: 1077-1085.
- 795 39. Cutler, S.R.,P.L. Rodriguez,R.R. Finkelstein, and S.R. Abrams, *Abscisic acid:*
796 *emergence of a core signaling network*. Annual Review of Plant Biology, 2010.
797 **61**: 651-679.
- 798 40. Takahashi, F.,T. Kuromori,H. Sato, and K. Shinozaki, *Regulatory gene*
799 *networks in drought stress responses and resistance in plants*. Survival

- 800 Strategies in Extreme Cold and Desiccation: Advances in Experimental
801 Medicine and Biology, 2018. **1081**: 189-214.
- 802 41. Yoshida, T.,J. Mogami, and K. Yamaguchi-Shinozaki, *ABA-dependent and*
803 *ABA-independent signaling in response to osmotic stress in plants*. Current
804 Opinion in Plant Biology, 2014. **21**: 133-139.
- 805 42. Barrero, J.M.,P.L. Rodriguez,V. Quesada,P. Piqueras,M.R. Ponce, and J.L.
806 Micol, *Both abscisic acid (ABA)-dependent and ABA-independent pathways*
807 *govern the induction of NCED3, AAO3 and ABA1 in response to salt stress*.
808 Plant, Cell & Environment, 2006. **29**: 2000-2008.
- 809 43. Waadt, R.,C.A. Seller,P.-K. Hsu,Y. Takahashi,S. Munemasa, and J.I.
810 Schroeder, *Plant hormone regulation of abiotic stress responses*. Nature
811 Reviews Molecular Cell Biology, 2022. **23**: 680-694.
- 812 44. Urano, K.,K. Maruyama,Y. Ogata,Y. Morishita,M. Takeda,N. Sakurai,H.
813 Suzuki,K. Saito,D. Shibata, and M. Kobayashi, *Characterization of the ABA-*
814 *regulated global responses to dehydration in Arabidopsis by metabolomics*. The
815 Plant Journal, 2009. **57**: 1065-1078.
- 816 45. Gervais, T.,A. Creelman,X.-Q. Li,B. Bizimungu,D. De Koeyer, and K. Dahal,
817 *Potato response to drought stress: Physiological and growth basis*. Frontiers in
818 plant science, 2021. **12**: 698060.
- 819 46. Aliche, E.B.,T.P. Theeuwen,M. Oortwijn,R.G. Visser, and C.G. van der Linden,
820 *Carbon partitioning mechanisms in potato under drought stress*. Plant
821 Physiology and Biochemistry, 2020. **146**: 211-219.
- 822 47. Serra Mari, R.,S. Schrunner,R. Finkers,F.M.R. Ziegler,P. Arens,M.H.W.
823 Schmidt,B. Usadel,G.W. Klau, and T. Marschall, *Haplotype-resolved assembly*

- 824 *of a tetraploid potato genome using long reads and low-depth offspring data.*
825 *Genome biology*, 2024. **25**: 26.
- 826 48. Hoopes, G.,X. Meng,J.P. Hamilton,S.R. Achakkagari,F.D.A.F. Guesdes,M.E.
827 Bolger,J.J. Coombs,D. Esselink,N.R. Kaiser,L. Kodde,M. Kyriakidou,B.
828 Lavrijssen,N. van Lieshout,R. Shereda,H.K. Tuttle,B. Vaillancourt,J.C.
829 Wood,J.M. de Boer,N. Bornowski,P. Bourke,D. Douches,H.J. van Eck,D.
830 Ellis,M.J. Feldman,K.M. Gardner,J.C.P. Hopman,J. Jiang,W.S. De Jong,J.C.
831 Kuhl,R.G. Novy,S. Oome,V. Sathuvalli,E.H. Tan,R.A. Ursum,M.I. Vales,K.
832 Vining,R.G.F. Visser,J. Vossen,G.C. Yench,N.L. Anglin,C.W.B. Bachem,J.B.
833 Endelman,L.M. Shannon,M.V. Strömvik,H.H. Tai,B. Usadel,C.R. Buell, and R.
834 Finkers, *Phased, chromosome-scale genome assemblies of tetraploid potato*
835 *reveal a complex genome, transcriptome, and predicted proteome landscape*
836 *underpinning genetic diversity*. *Molecular Plant*, 2022. **15**: 520-536.
- 837 49. Harris, P.M., *The potato crop: the scientific basis for improvement*. 1992,
838 London: Chapman and Hall.
- 839 50. Hou, J.,H. Zhang,J. Liu,S. Reid,T. Liu,S. Xu,Z. Tian,U. Sonnewald,B. Song,
840 and C. Xie, *Amylases StAmy23, StBAM1 and StBAM9 regulate cold-induced*
841 *sweetening of potato tubers in distinct ways*. *Journal of Experimental Botany*,
842 2017. **68**: 2317-2331.
- 843 51. Sowokinos, J.R., *Biochemical and molecular control of cold-induced*
844 *sweetening in potatoes*. *American Journal of Potato Research*, 2001. **78**: 221-
845 236.
- 846 52. Wismer, W.,A. Marangoni, and R. Yada, *Low-temperature sweetening in roots*
847 *and tubers*. *Horticultural Reviews*, 1995. **17**: 203-231.

- 848 53. Koch, K., *Sucrose metabolism: regulatory mechanisms and pivotal roles in*
849 *sugar sensing and plant development*. Current Opinion in Plant Biology, 2004.
850 7: 235-246.
- 851 54. Zhang, H.,J. Liu,J. Hou,Y. Yao,Y. Lin,Y. Ou,B. Song, and C. Xie, *The potato*
852 *amylase inhibitor gene Sb AI regulates cold-induced sweetening in potato*
853 *tubers by modulating amylase activity*. Plant biotechnology journal, 2014. **12**:
854 984-993.
- 855 55. Lin, Y.,T. Liu,J. Liu,X. Liu,Y. Ou,H. Zhang,M. Li,U. Sonnewald,B. Song, and
856 C. Xie, *Subtle regulation of potato acid invertase activity by a protein complex*
857 *of invertase, invertase inhibitor, and sucrose nonfermenting1-related protein*
858 *kinase*. Plant Physiology, 2015. **168**: 1807-1819.
- 859 56. Zhu, X.,C. Richael,P. Chamberlain,J.S. Busse,A.J. Bussan,J. Jiang, and P.C.
860 Bethke, *Vacuolar invertase gene silencing in potato (Solanum tuberosum L.)*
861 *improves processing quality by decreasing the frequency of sugar-end defects*.
862 PloS one, 2014. **9**: e93381.
- 863 57. Abbott, W.S., *A method of computing the effectiveness of an insecticide*. Journal
864 Economic Entomology, 1925. **18**: 265-267.
- 865 58. Dalal, A.,R. Bourstein,N. Haish,I. Shenhar,R. Wallach, and M. Moshelion,
866 *Dynamic physiological phenotyping of drought-stressed pepper plants treated*
867 *with “productivity-enhancing” and “survivability-enhancing” biostimulants*.
868 Frontiers in plant science, 2019. **10**: 905.
- 869 59. Lawson, T. and M.R. Blatt, *Stomatal Size, Speed, and Responsiveness Impact*
870 *on Photosynthesis and Water Use Efficiency* Plant Physiology, 2014. **164**:
871 1556-1570.

- 872 60. Flexas, J.,Ü. Niinemets,A. Gallé,M.M. Barbour,M. Centritto,A. Diaz-Espejo,C.
873 Douthe,J. Galmés,M. Ribas-Carbo,P.L. Rodriguez,F. Rosselló,R.
874 Soolanayakanahally,M. Tomas,I.J. Wright,G.D. Farquhar, and H. Medrano,
875 *Diffusional conductances to CO₂ as a target for increasing photosynthesis and*
876 *photosynthetic water-use efficiency*. *Photosynthesis Research*, 2013. **117**: 45-
877 59.
- 878 61. Henry, C. and G.P. John, *A stomatal safety-efficiency trade-off constrains*
879 *responses to leaf dehydration*. *Nature communications*, 2019. **10**: 3398.
- 880 62. Sengupta, S.,S. Mukherjee,P. Basak, and A.L. Majumder, *Significance of*
881 *galactinol and raffinose family oligosaccharide synthesis in plants*. *Frontiers in*
882 *plant science*, 2015. **6**: 656.
- 883 63. Urban, J.,M.W. Ingwers,M.A. McGuire, and R.O. Teskey, *Increase in leaf*
884 *temperature opens stomata and decouples net photosynthesis from stomatal*
885 *conductance in Pinus taeda and Populus deltoides x nigra*. *Journal of*
886 *Experimental Botany*, 2017. **68**: 1757-1767.
- 887 64. Suzuki, N.,S. Koussevitzky,R. Mittler, and G. Miller, *ROS and redox signalling*
888 *in the response of plants to abiotic stress*. *Plant Cell Environ*, 2012. **35**: 259-70.
- 889 65. Zhang, F.,T. Li,L. Gao,D. Elango,J. Song,C. Su,M. Li,W. Zhang,M. Chi,X.
890 Wang, and Y. Wu, *Correlation analysis of transcriptome and metabolomics and*
891 *functional study of Galactinol synthase gene (VcGolS3) of blueberry under salt*
892 *stress*. *Plant Molecular Biology*, 2025. **115**: 27.
- 893 66. Zhu, M.,R. Xiao,T. Yu,T. Guo,X. Zhong,J. Qu,W. Du, and W. Xue, *Raffinose*
894 *Priming Improves Seed Vigor by ROS Scavenging, RAFS, and α-GAL Activity*
895 *in Aged Waxy Corn*. *Agronomy*, 2024. **14**: 2843.

- 896 67. Teper-Bamnolker, P.,M. Roitman,O. Katar,N. Peleg,K. Aruchamy,S. Suher,A.
897 Doron-Faigenboim,D. Leibman,A. Omid,E. Belausov,M. Andersson,N.
898 Olsson,A.-S. Fält,H. Volpin,P. Hofvander,A. Gal-On, and D. Eshel, *An*
899 *alternative pathway to plant cold tolerance in the absence of vacuolar invertase*
900 *activity*. The Plant Journal, 2023. **113**: 327-341.
- 901 68. Flexas, J.,M. Ribas-Carbó,A. Diaz-Espejo,J. Galmés, and H. Medrano,
902 *Mesophyll conductance to CO₂: current knowledge and future prospects*. Plant
903 Cell Environ, 2008. **31**: 602-21.
- 904 69. Tomás, M.,J. Flexas,L. Copolovici,J. Galmés,L. Hallik,H. Medrano,M. Ribas-
905 Carbó,T. Tosens,V. Vislap, and Ü. Niinemets, *Importance of leaf anatomy in*
906 *determining mesophyll diffusion conductance to CO₂ across species:*
907 *quantitative limitations and scaling up by models*. Journal of Experimental
908 Botany, 2013. **64**: 2269-2281.
- 909 70. Flexas, J.,M.M. Barbour,O. Brendel,H.M. Cabrera,M. Carriquí,A. Díaz-
910 Espejo,C. Douthe,E. Dreyer,J.P. Ferrio,J. Gago,A. Gallé,J. Galmés,N.
911 Kodama,H. Medrano,Ü. Niinemets,J.J. Peguero-Pina,A. Pou,M. Ribas-
912 Carbó,M. Tomás,T. Tosens, and C.R. Warren, *Mesophyll diffusion conductance*
913 *to CO₂: an unappreciated central player in photosynthesis*. Plant Science, 2012.
914 **193-194**: 70-84.
- 915 71. Fleta-Soriano, E. and S. Munné-Bosch, *Stress Memory and the Inevitable*
916 *Effects of Drought: A Physiological Perspective*. Frontiers in plant science,
917 2016. **Volume 7 - 2016**.
- 918 72. Hilker, M.,J. Schwachtje,M. Baier,S. Balazadeh,I. Bäurle,S. Geiselhardt,D.K.
919 Hinch,R. Kunze,B. Mueller-Roeber,M.C. Rillig,J. Rolff,T. Romeis,T.
920 Schmülling,A. Steppuhn,J. van Dongen,S.J. Whitcomb,S. Wurst,E. Zuther, and

- 921 J. Kopka, *Priming and memory of stress responses in organisms lacking a*
922 *nervous system*. Biol Rev Camb Philos Soc, 2016. **91**: 1118-1133.
- 923 73. Sweetlove, L.J.,K.F.M. Beard,A. Nunes-Nesi,A.R. Fernie, and R.G. Ratcliffe,
924 *Not just a circle: flux modes in the plant TCA cycle*. Trends in Plant Science,
925 2010. **15**: 462-470.
- 926 74. Nishizawa, A.,Y. Yabuta, and S. Shigeoka, *Galactinol and Raffinose Constitute*
927 *a Novel Function to Protect Plants from Oxidative Damage* Plant Physiology,
928 2008. **147**: 1251-1263.
- 929 75. Sengupta, S.,S. Mukherjee,P. Basak, and A.L. Majumder, *Significance of*
930 *galactinol and raffinose family oligosaccharide synthesis in plants*. Front Plant
931 Sci, 2015. **Volume 6 - 2015**.
- 932 76. Yan, S.,L. Qing,L. Wenyan,Y. Jianbing, and A.R. and Fernie, *Raffinose Family*
933 *Oligosaccharides: Crucial Regulators of Plant Development and Stress*
934 *Responses*. Critical reviews in plant sciences, 2022. **41**: 286-303.
- 935 77. Wingler, A., *Transitioning to the Next Phase: The Role of Sugar Signaling*
936 *throughout the Plant Life Cycle*. Plant Physiology, 2017. **176**: 1075-1084.
- 937 78. Taji, T.,C. Ohsumi,S. Iuchi,M. Seki,M. Kasuga,M. Kobayashi,K. Yamaguchi-
938 Shinozaki, and K. Shinozaki, *Important roles of drought- and cold-inducible*
939 *genes for galactinol synthase in stress tolerance in Arabidopsis thaliana*. The
940 Plant Journal, 2002. **29**: 417-426.
- 941 79. Zia, R.,M.S. Nawaz,M.J. Siddique,S. Hakim, and A. Imran, *Plant survival*
942 *under drought stress: Implications, adaptive responses, and integrated*
943 *rhizosphere management strategy for stress mitigation*. Microbiological
944 Research, 2021. **242**: 126626.

- 945 80. Zheng, D.,M. Fu,C. Sun,Q. Yang,X. Zhang,J. Lu,M. Chang,L. Liu,X. Wan, and
946 Q. Chen, *CsABF8 mediates drought-induced ABA signaling in the regulation of*
947 *raffinose biosynthesis in Camellia sinensis leaves*. International Journal of
948 Biological Macromolecules, 2025. **311**: 143521.
- 949 81. Van den Ende, W. and R. Valluru, *Sucrose, sucrosyl oligosaccharides, and*
950 *oxidative stress: scavenging and salvaging?* Journal of Experimental Botany,
951 2008. **60**: 9-18.
- 952 82. Rolland, F.,E. Baena-Gonzalez, and J. Sheen, *SUGAR SENSING AND*
953 *SIGNALING IN PLANTS: Conserved and Novel Mechanisms*. Annual Review
954 of Plant Biology, 2006. **57**: 675-709.
- 955 83. Rook, F.,F. Corke,R. Card,G. Munz,C. Smith, and M.W. Bevan, *Impaired*
956 *sucrose-induction mutants reveal the modulation of sugar-induced starch*
957 *biosynthetic gene expression by abscisic acid signalling*. The Plant Journal,
958 2001. **26**: 421-433.
- 959 84. Haghpanah, M.,S. Hashemipetroudi,A. Arzani, and F. Araniti, *Drought*
960 *tolerance in plants: Physiological and molecular responses*. Plants (Basel),
961 2024. **13**.
- 962 85. Sanyal, R.,S. Kumar,A. Pattanayak,A. Kar, and S.K. Bishi, *Optimizing raffinose*
963 *family oligosaccharides content in plants: A tightrope walk*. Frontiers in Plant
964 Science, 2023. **Volume 14 - 2023**.
- 965 86. Horacio, P. and G. and Martinez-Noel, *Sucrose signaling in plants: A world yet*
966 *to be explored*. Plant Signaling & Behavior, 2013. **8**: e23316.
- 967 87. Ramel, F.,C. Sulmon,M. Bogard,I. Couée, and G. Gouesbet, *Differential*
968 *patterns of reactive oxygen species and antioxidative mechanisms during*

- 969 *atrazine injury and sucrose-induced tolerance in Arabidopsis thaliana*
970 *plantlets*. BMC Plant Biology, 2009. **9**: 28.
- 971 88. Berg, J.,C.M. Rodrigues,C. Scheid,Y. Pirrotte,C. Picco,J. Scholz-Starke,W.
972 Zierer,O. Czarnecki,D. Hackenberg,F. Ludewig,W. Koch,H.E. Neuhaus,C.
973 Müdsam,B. Pommerrenig, and I. Keller, *The Vacuolar Inositol Transporter*
974 *BvINT1;1 Contributes to Raffinose Biosynthesis and Reactive Oxygen Species*
975 *Scavenging During Cold Stress in Sugar Beet*. Plant, Cell & Environment, 2025.
976 **48**: 3471-3486.
- 977 89. Zulfiqar, F. and M. Ashraf, *Proline Alleviates Abiotic Stress Induced Oxidative*
978 *Stress in Plants*. Journal of Plant Growth Regulation, 2023. **42**: 4629-4651.
- 979 90. Szabados, L. and A. Savouré, *Proline: a multifunctional amino acid*. Trends in
980 Plant Science, 2010. **15**: 89-97.
- 981 91. KAVI KISHOR, P.B. and N. SREENIVASULU, *Is proline accumulation per*
982 *se correlated with stress tolerance or is proline homeostasis a more critical*
983 *issue?* Plant, Cell & Environment, 2014. **37**: 300-311.
- 984 92. Sade, N.,A. Gebremedhin, and M. Moshelion, *Risk-taking plants: anisohydric*
985 *behavior as a stress-resistance trait*. Plant Signaling & Behavior, 2012. **7**: 767-
986 770.
- 987 93. McAdam, S.A.M. and T.J. Brodribb, *Mesophyll Cells Are the Main Site of*
988 *Abscisic Acid Biosynthesis in Water-Stressed Leaves*. 2018. **177**: 911-917.
- 989 94. Gong, L.,X.D. Liu,Y.Y. Zeng,X.Q. Tian,Y.L. Li, and N.C. Turner, *Stomatal*
990 *morphology and physiology explain varied sensitivity to abscisic acid across*
991 *vascular plant lineages*. Plant Physiology, 2021. **186**: 782-797.

- 992 95. Hasan, M.M.,L. Gong,Z.-F. Nie,F.-P. Li,G.J. Ahammed, and X.-W. Fang, *ABA-*
993 *induced stomatal movements in vascular plants during dehydration and*
994 *rehydration*. Environmental and experimental botany, 2021. **186**: 104436.
- 995 96. Cutler, S.R.,P.L. Rodriguez,R.R. Finkelstein, and S.R. Abrams, *Abscisic acid:*
996 *emergence of a core signaling network*. Annu Rev Plant Biol, 2010. **61**: 651-
997 79.
- 998 97. Fujita, Y.,M. Fujita,K. Shinozaki, and K. Yamaguchi-Shinozaki, *ABA-mediated*
999 *transcriptional regulation in response to osmotic stress in plants*. Journal of
1000 Plant Research, 2011. **124**: 509-525.
- 1001 98. Mega, R.,F. Abe,J.-S. Kim,Y. Tsuboi,K. Tanaka,H. Kobayashi,Y. Sakata,K.
1002 Hanada,H. Tsujimoto,J. Kikuchi,S.R. Cutler, and M. Okamoto, *Tuning water-*
1003 *use efficiency and drought tolerance in wheat using abscisic acid receptors*.
1004 Nature Plants, 2019. **5**: 153-159.
- 1005 99. Granot, D.,R. David-Schwartz, and G. Kelly, *Hexose Kinases and Their Role in*
1006 *Sugar-Sensing and Plant Development*. Frontiers in Plant Science, 2013.
1007 **Volume 4 - 2013**.
- 1008 100. Verslues, P.E. and T.E. Juenger, *Drought, metabolites, and Arabidopsis natural*
1009 *variation: a promising combination for understanding adaptation to water-*
1010 *limited environments*. Current Opinion in Plant Biology, 2011. **14**: 240-245.
- 1011 101. Ahmad, F.,A. Singh, and A. Kamal, *Osmoprotective Role of Sugar in Mitigating*
1012 *Abiotic Stress in Plants*, in *Protective Chemical Agents in the Amelioration of*
1013 *Plant Abiotic Stress*. 2020. p. 53-70.
- 1014 102. Sakr, S.,M. Wang,F. Dédaldéchamp,M.-D. Perez-Garcia,L. Ogé,L. Hamama,
1015 and R. Atanassova, *The Sugar-Signaling Hub: Overview of Regulators and*

- 1016 *Interaction with the Hormonal and Metabolic Network*. International Journal of
1017 Molecular Sciences, 2018. **19**: 2506.
- 1018 103. Kravchenko, A.,S. Citerne,I. Jéhanno,R.I. Bersimbaev,B. Veit,C. Meyer, and
1019 A.-S. Leprince, *Mutations in the Arabidopsis Lst8 and Raptor genes encoding*
1020 *partners of the TOR complex, or inhibition of TOR activity decrease abscisic*
1021 *acid (ABA) synthesis*. Biochemical and biophysical research communications,
1022 2015. **467**: 992-997.
- 1023 104. Huijser, C.,A. Kortstee,J. Pego,P. Weisbeek,E. Wisman, and S. Smeeckens, *The*
1024 *Arabidopsis SUCROSE UNCOUPLED-6 gene is identical to ABSCISIC ACID*
1025 *INSENSITIVE-4: involvement of abscisic acid in sugar responses*. The Plant
1026 Journal, 2000. **23**: 577-85.
- 1027 105. Engineer, C.B.,M. Hashimoto-Sugimoto,J. Negi,M. Israelsson-Nordström,T.
1028 Azoulay-Shemer,W.-J. Rappel,K. Iba, and J.I. Schroeder, *CO₂*
1029 *Sensing and CO₂ Regulation of Stomatal Conductance:*
1030 *Advances and Open Questions*. Trends in Plant Science, 2016. **21**: 16-30.
- 1031 106. Dalal, A.,I. Shenhar,R. Bourstein,A. Mayo,Y. Grunwald,N. Averbuch,Z.
1032 Attia,R. Wallach, and M. Moshelion, *A Telemetric, Gravimetric Platform for*
1033 *Real-Time Physiological Phenotyping of Plant-Environment Interactions*. J Vis
1034 Exp, 2020.
- 1035 107. Gosa, S.C.,A. Koch,I. Shenhar,J. Hirschberg,D. Zamir, and M. Moshelion, *The*
1036 *potential of dynamic physiological traits in young tomato plants to predict field-*
1037 *yield performance*. Plant Science, 2022. **315**: 111122.
- 1038 108. Halperin, O.,A. Gebremedhin,R. Wallach, and M. Moshelion, *High-throughput*
1039 *physiological phenotyping and screening system for the characterization of*
1040 *plant-environment interactions*. The Plant Journal, 2017. **89**: 839-850.

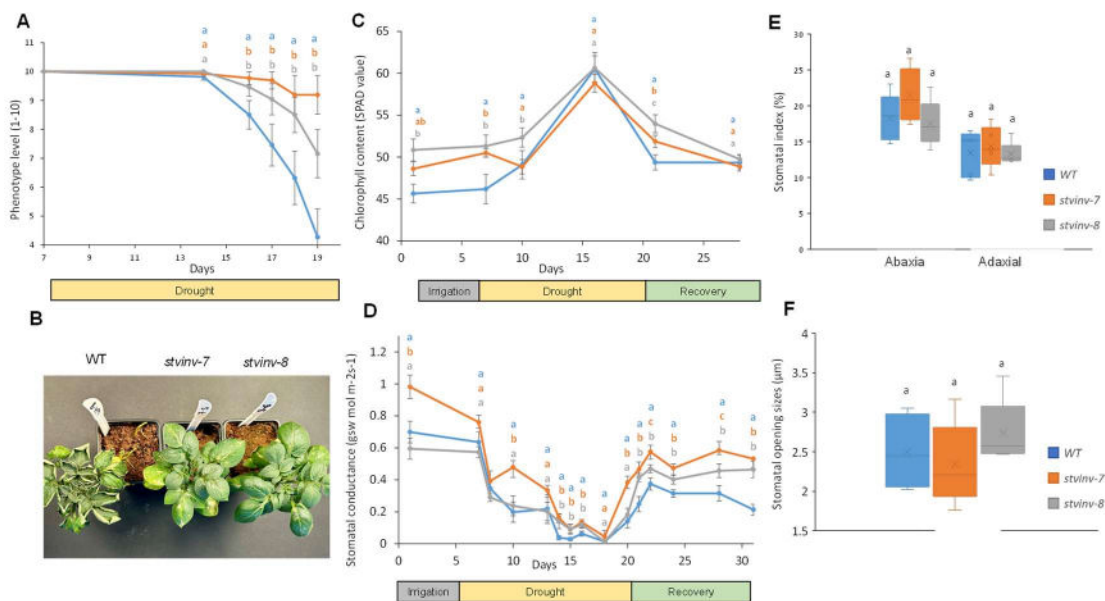
- 1041 109. Galkin, E.,A. Dalal,A. Evenko,E. Fridman,I. Kan,R. Wallach, and M.
1042 Moshelion, *Risk-management strategies and transpiration rates of wild barley*
1043 *in uncertain environments*. *Physiologia Plantarum*, 2018. **164**: 412-428.
- 1044 110. Paul, M.,J. Tanskanen,M. Jääskeläinen,W. Chang,A. Dalal,M. Moshelion, and
1045 A.H. Schulman, *Drought and recovery in barley: key gene networks and*
1046 *retrotransposon response*. *Frontiers in plant science*, 2023. **14**: 1193284.
- 1047 111. Danieli, R.,S. Assouline,B.B. Salam,O. Vrobel,P. Teper-Bamnlker,E.
1048 Belausov,D. Granot,P. Tarkowski, and D. Eshel, *Chilling induces sugar and*
1049 *ABA accumulation that antagonistically signals for symplastic connection of*
1050 *dormant potato buds*. *Plant, Cell & Environment*, 2023. **46**: 2097-2111.
- 1051 112. Vrobel, O.,S. Čavar Zeljković,J. Dehner,L. Spíchal,N. De Diego, and P.
1052 Tarkowski, *Multi-class plant hormone HILIC-MS/MS analysis coupled with*
1053 *high-throughput phenotyping to investigate plant–environment interactions*.
1054 *The Plant Journal*, 2024. **120**: 818-832.
- 1055 113. Pang, Z.,J. Chong,G. Zhou,D.A. de Lima Morais,L. Chang,M. Barrette,C.
1056 Gauthier,P.E. Jacques,S. Li, and J. Xia, *MetaboAnalyst 5.0: narrowing the gap*
1057 *between raw spectra and functional insights*. *Nucleic Acids Res*, 2021. **49**:
1058 W388-W396.
- 1059 114. Geisler, M.J. and F.D. Sack, *Variable timing of developmental progression in*
1060 *the stomatal pathway in Arabidopsis cotyledons*. *New Phytologist*, 2002. **153**:
1061 469-476.
- 1062 115. Geisler, M.,J. Nadeau, and F.D. Sack, *Oriented asymmetric divisions that*
1063 *generate the stomatal spacing pattern in Arabidopsis are disrupted by the too*
1064 *many mouths mutation*. *The Plant Cell*, 2000. **12**: 2075-2086.

1065 116. Schneider, C.A., W.S. Rasband, and K.W. Eliceiri, *NIH Image to ImageJ: 25*
1066 *years of image analysis*. Nature Methods, 2012. 9: 671-675.

1067

1068

1069 Figure legends:



1070

1071 **Fig. 1. *stvinv* plants show resilient phenotypes under drought conditions with**

1072 **higher chlorophyll content and stomatal conductance.** Potato plants of wild type

1073 (WT) and *stvinv* lines (*stvinv-7*, and *stvinv-8*) were grown under controlled conditions

1074 with a 16-hour photoperiod at 23°C and then subjected to drought treatment (days 15-

1075 19), and irrigated again until full recovery. **A**, Phenotype visual score during drought

1076 treatment. **B**, representative plants at the end of the drought treatment. **C**, Changes in

1077 chlorophyll content; **D**, Leaf stomatal conductance. Different letters above data points

1078 indicate statistically significant differences between genotypes ($p < 0.05$). **E**, Stomatal

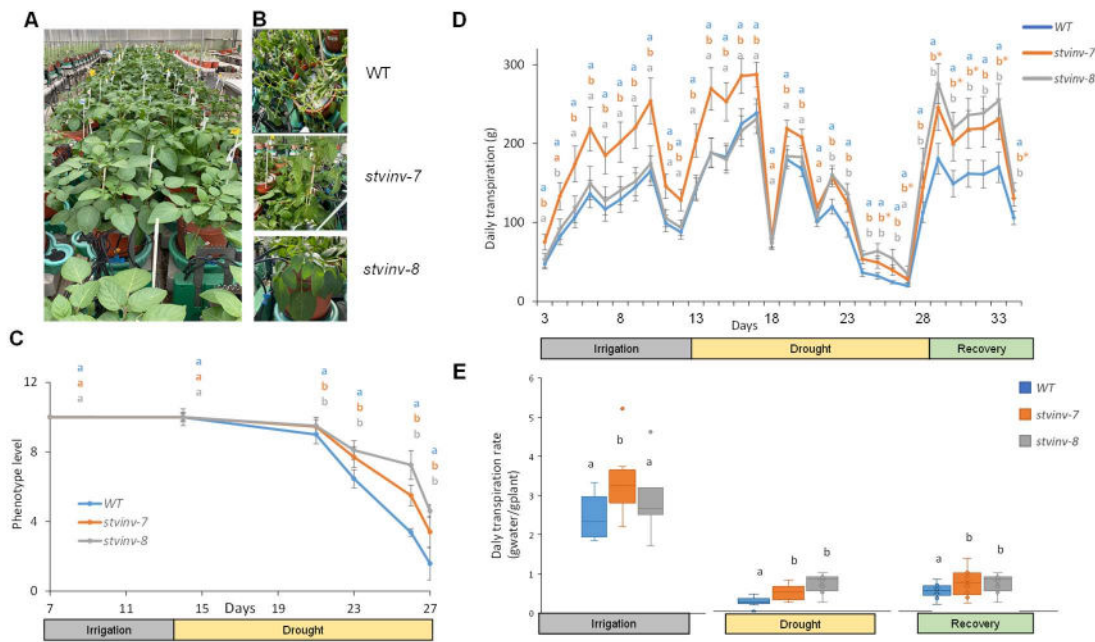
1079 index calculated as the ratio of stomatal number to total epidermal cells, with stomatal

1080 density (number of stomata per mm²) quantified by counting stomata in calibrated

1081 microscopic fields. **F**, Stomatal opening size (aperture width) measured from epidermal

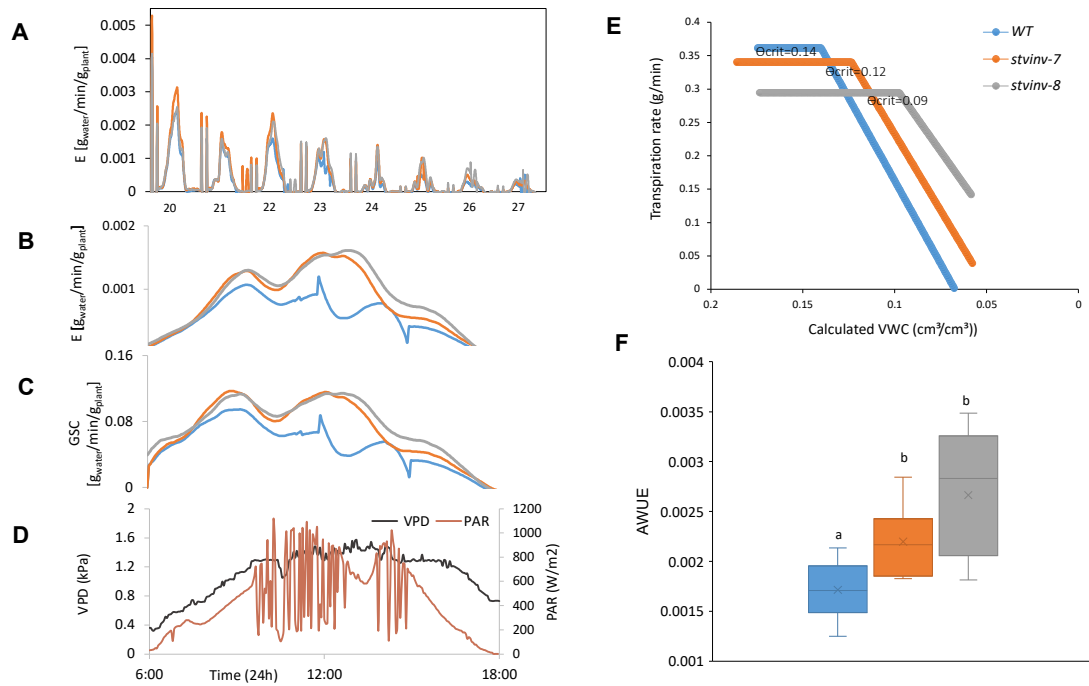
1082 peels using light microscopy and analyzed with ImageJ software.

1083



1084

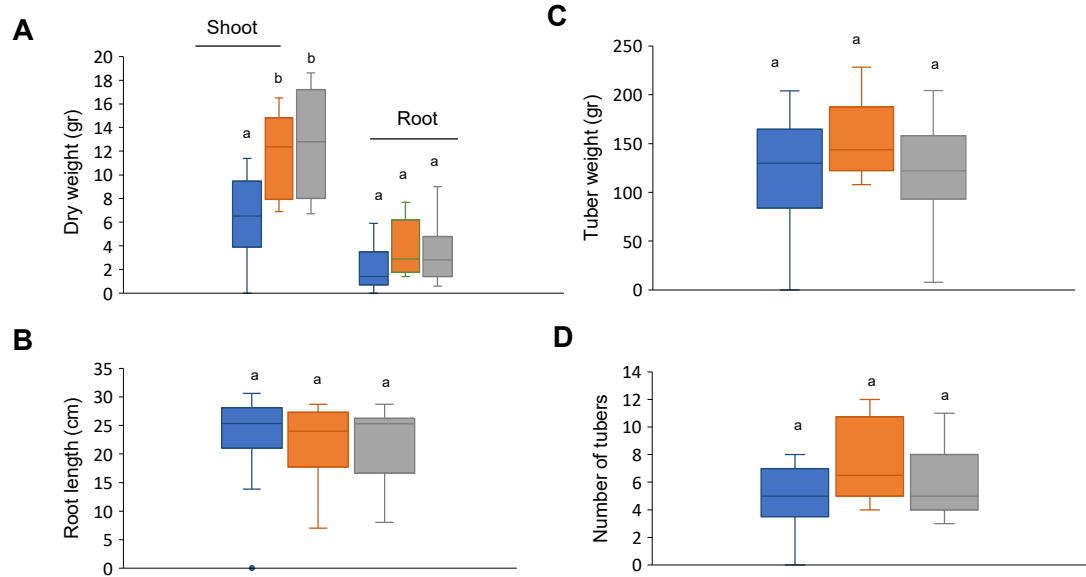
1085 **Fig. 2. *stinv* plants demonstrate enhanced drought tolerance.** A, Experimental
1086 design using PlantArray 3.0. Plants were placed on load cells for continuous monitoring
1087 of transpiration and conductance. Drought stress was initiated on day 13 for a subset,
1088 followed by rehydration on day 27; controls remained well-irrigated throughout. B,
1089 Representative images of plants on day 25 (corresponding to day 13 of drought),
1090 highlighting genotype-specific responses. C, Phenotypic assessment of plant vigor
1091 during drought and recovery (scale 1–10; 1 = severe wilting, 10 = fully vigorous). D,
1092 Whole-plant daily transpiration rates across irrigation (days 1–12), drought (days 13–
1093 27), and recovery (days 28–34). E, Normalized whole-plant daily transpiration rates
1094 (per unit biomass). Different letters above data points indicate statistically significant
1095 differences between genotypes ($p < 0.05$).



1096

1097 **Fig. 3. Physiological responses of WT and *stinv* plants under drought conditions.**

1098 **A**, Whole-canopy normalized transpiration rates (E) of WT, *stinv-7*, and *stinv-8*
1099 monitored continuously during the drought period (days 20–27) between 06:00 and
1100 18:00, under natural photosynthetically active radiation (PAR) and vapor pressure
1101 deficit (VPD). **B**, Daily variation in environmental conditions on a representative
1102 drought day (day 23), showing PAR (red) and VPD (black). **C**, Whole-canopy stomatal
1103 conductance (GSC) measured continuously on day 23. **D**, Whole-canopy transpiration
1104 rates (E) on day 23. **E**, Critical soil water content (Θ_{crit}), defined as the volumetric
1105 water content (VWC) at which transpiration is restricted. **F**, Agronomic water-use
1106 efficiency (AWUE), calculated as shoot dry weight per total water transpired. Boxplots
1107 show medians, interquartile ranges, and individual values. Different letters indicate
1108 statistically significant differences ($p < 0.05$). Error bars represent \pm SE; $n = 10$ –13 per
1109 group.

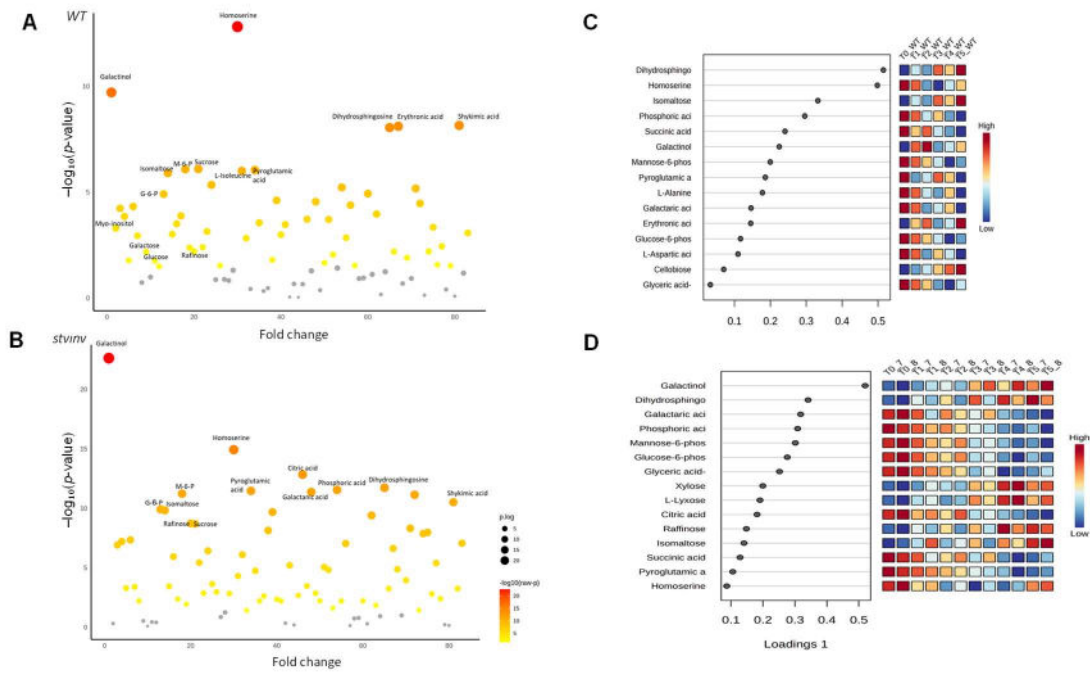


1110

1111 **Fig. 4. Enhanced biomass and tuber yield in *stvinv-7* and *stvinv-8* plants under**
1112 **drought conditions. A, Shoot dry weight, B, root dry weight, C, number of tubers, D,**
1113 **total tuber weight, and E, tuber size were measured at harvest (day 34) and are presented**
1114 **as box-and-whisker plots. Different letters indicate statistically significant differences**
1115 **between genotypes (Student's t-test, $p < 0.05$). $n = 10-13$ plants per group.**

1116

1117



1118

1119 **Fig. 5. Divergent metabolic responses to drought stress in WT and *stvinv* plants.**

1120 **A-B**, Volcano plots showing drought-induced changes in metabolite abundance for WT

1121 (A) and *stvinv* plants (B). The x-axis indicates fold change; the y-axis shows $-\log_{10}(p$ -

1122 value). Larger bubbles and warmer colors (yellow to red) represent metabolites with

1123 greater statistical significance. Only metabolites with $p < 0.05$ (ANOVA with post hoc

1124 tests) are shown. **C-D**, Sparse PLS-DA of leaf metabolite profiles across drought stages

1125 (T0, irrigation; T1–T2, early drought; T3, mid-drought; T4–T5, severe

1126 drought/recovery) in WT (C) and *stvinv* plants (D). For each genotype, the dot plot

1127 shows the loadings of metabolites on component 1, indicating their contribution to

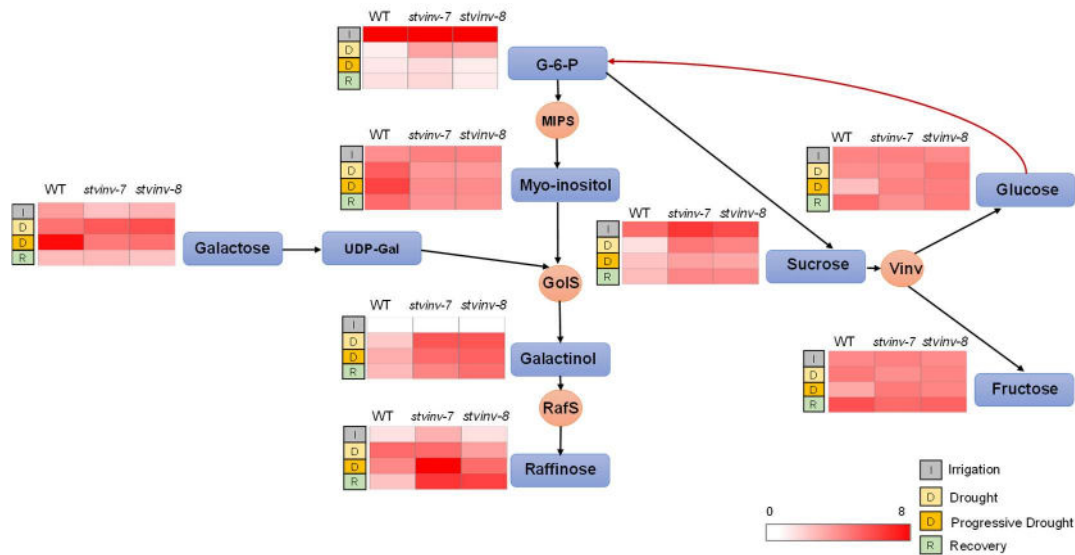
1128 separation among drought stages, and the adjacent heatmap shows their scaled

1129 abundance across time points and biological replicates, illustrating a shift from amino-

1130 acid and sphingolipid associated markers in WT to persistent enrichment of galactinol,

1131 raffinose and related sugars in *stvinv*.

1132



1133

1134 **Fig. 6. Schematic overview of raffinose family oligosaccharide (RFO) metabolism**

1135 **in WT and *stvinv* plants across irrigation, drought, and recovery phases.**

1136 The diagram illustrates key metabolites involved in the RFO pathway, including

1137 glucose-6-phosphate (G-6-P), glucose, fructose, sucrose, galactose, UDP-galactose,

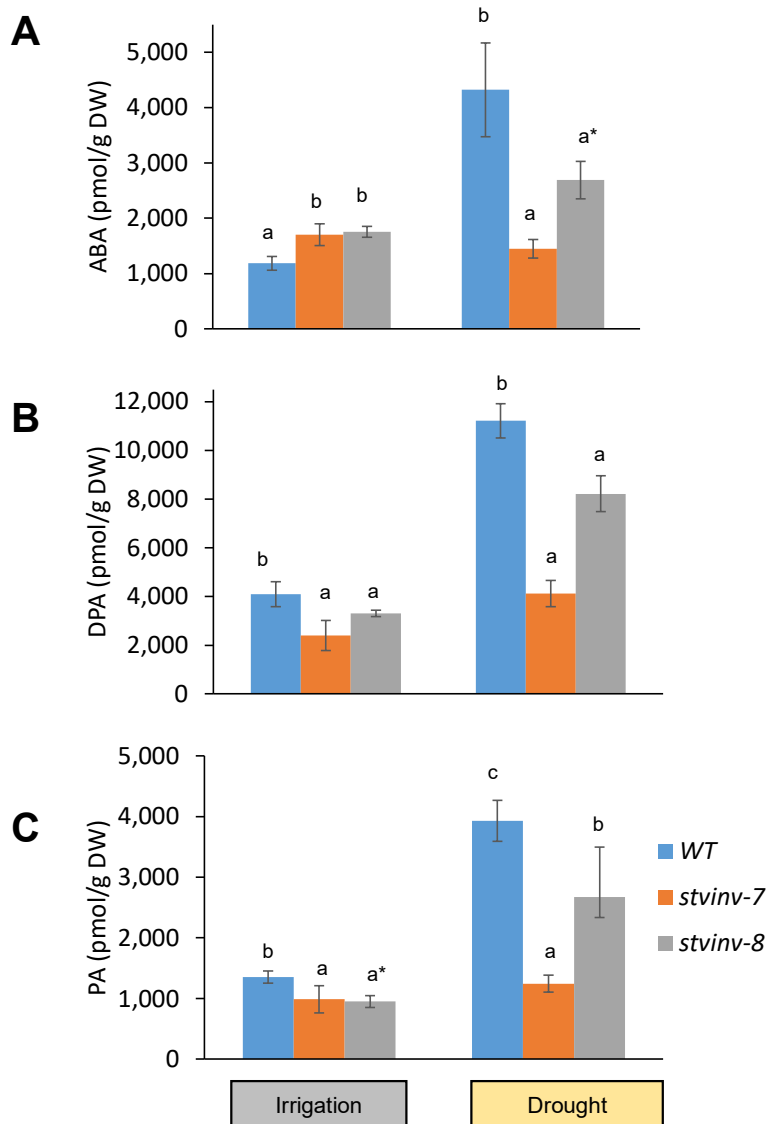
1138 myo-inositol, galactinol, and raffinose. Metabolic conversions are indicated by arrows

1139 and associated enzymes: myo-inositol phosphate synthase (MIPS), galactinol synthase

1140 (GoIS), raffinose synthase (RafS), and vacuolar invertase (VInv). Adjacent heatmaps

1141 represent the relative abundance of each metabolite in WT, *stvinv-7*, and *stvinv-8* under

1142 irrigation (I), drought (D), and recovery (R) conditions (darker red = higher abundance).



1143

1144 **Fig. 7. Reduced ABA accumulation and catabolism in *stvinv* plants under drought**

1145 **stress.** A–C, Concentrations of abscisic acid (ABA), phaseic acid (PA), and

1146 dehydrophaseic acid (DPA) were quantified in WT, *stvinv-7*, and *stvinv-8* plants under

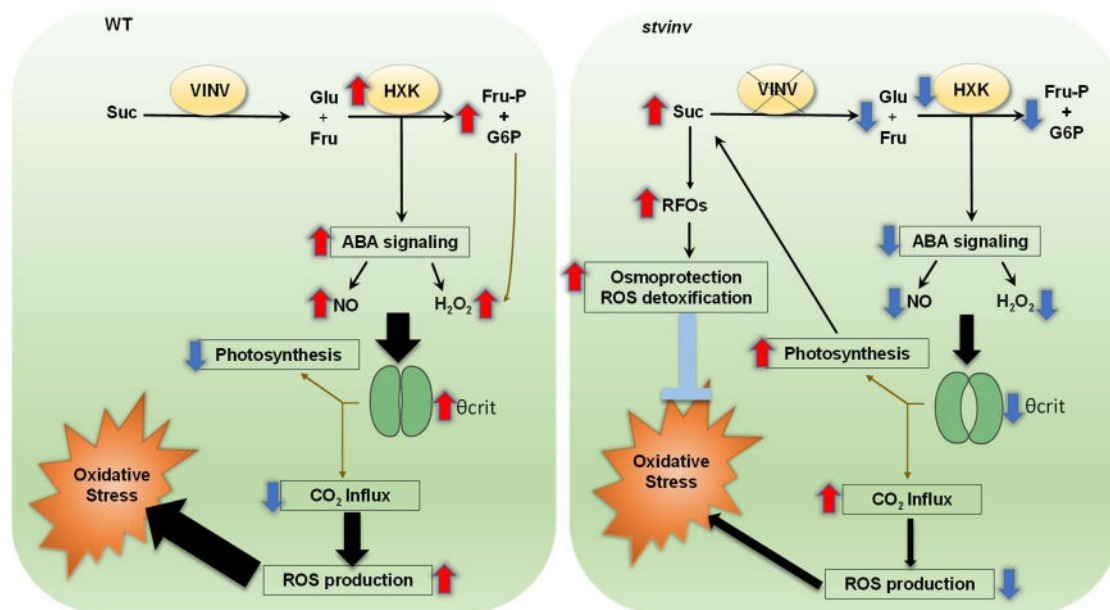
1147 irrigation and after 7 days of drought using LC-MS. Hormone levels are presented as

1148 pmol/g dry weight (DW). Data represent means \pm SE ($n = 5-6$ plants per group).

1149 Different letters denote statistically significant differences between genotypes within

1150 each treatment (Student's *t*-test, $p < 0.05$); asterisks (*) indicate marginal significance

1151 ($p = 0.05-0.1$).



1152

1153 **Fig. 8. Proposed mechanistic model for enhanced drought tolerance in *stvinv***

1154 **plants.** Schematic model illustrating the differential metabolic and signaling responses

1155 to drought stress in WT and *stvinv* plants. In WT plants (left panel), sucrose is cleaved

1156 by vacuolar invertase (VINV) into glucose (Glu) and fructose (Fru). These hexoses are

1157 phosphorylated by hexokinase (HXK), leading to the accumulation of fructose-6-

1158 phosphate (Fru-P) and glucose-6-phosphate (G6P). HXK-mediated sugar signaling

1159 enhances abscisic acid (ABA) signaling and increases the production of nitric oxide

1160 (NO) and hydrogen peroxide (H₂O₂). This signaling cascade drives stomatal closure at

1161 the critical threshold (θ_{crit}), reduces CO₂ influx, and decreases photosynthetic activity.

1162 In parallel, enhanced ROS production amplifies oxidative stress and ultimately

1163 compromises drought resilience. In *stvinv* plants (right panel), suppression of vacuolar

1164 invertase activity results in sucrose accumulation and enhanced synthesis of raffinose

1165 family oligosaccharides (RFOs). These sugars provide osmoprotection and facilitate

1166 ROS detoxification, thereby alleviating oxidative stress. Attenuated HXK activity

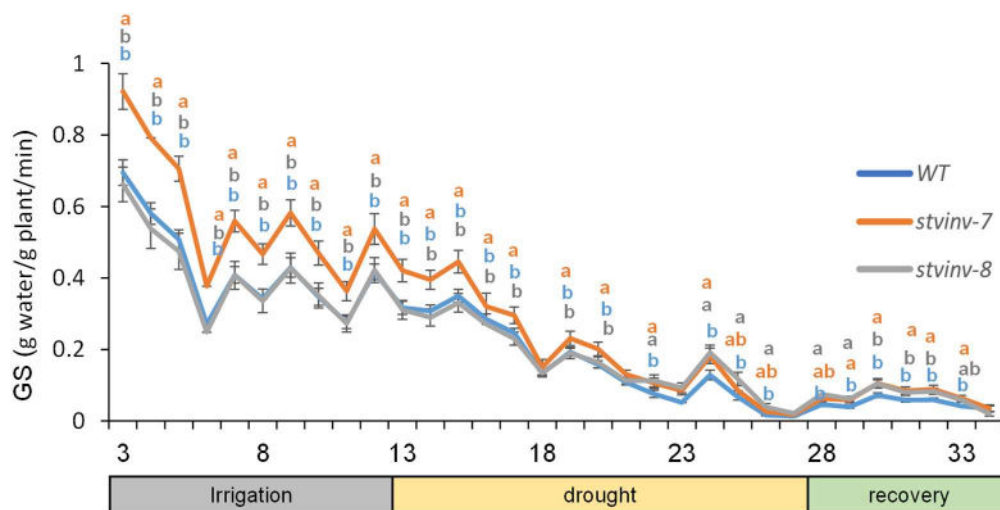
1167 reduces ABA-dependent signaling, leading to lower NO and H₂O₂ levels and

1168 consequently a weaker induction of stomatal closure. As a result, CO₂ influx is

1169 maintained, photosynthesis remains higher, and ROS production is suppressed.
1170 Together, these responses underlie the superior drought tolerance of *stvinv* plants. In
1171 the diagram, red upward arrows indicate increases, blue downward arrows indicate
1172 decreases, blue T-shaped bars denote inhibitory effects, thick black arrows highlight
1173 major stress-related fluxes toward ROS generation and oxidative damage, thin arrows
1174 represent direct metabolic and regulatory connections, and brown arrows indicate
1175 indirect regulatory pathways such as HXK-mediated effects on ABA signaling.

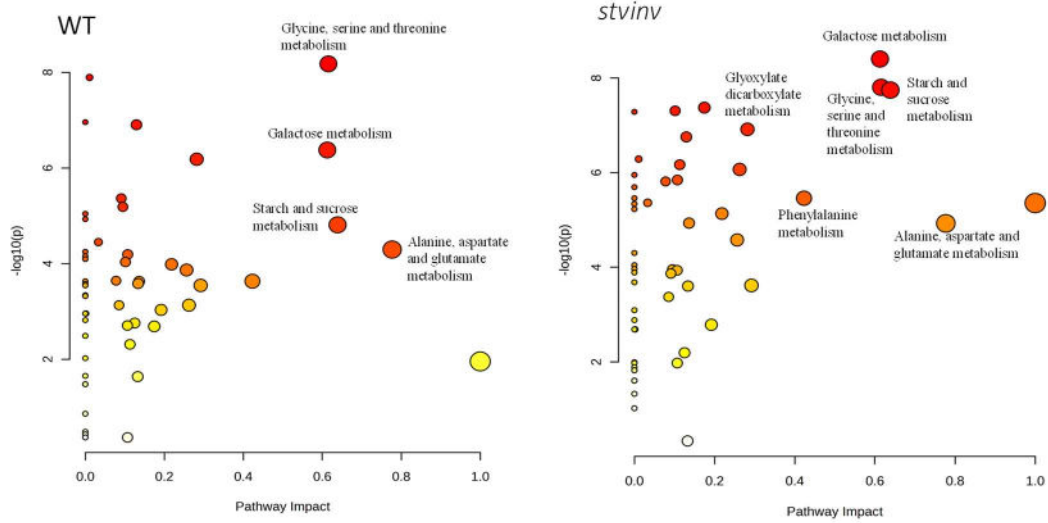
1176

1177 Supplementary figures



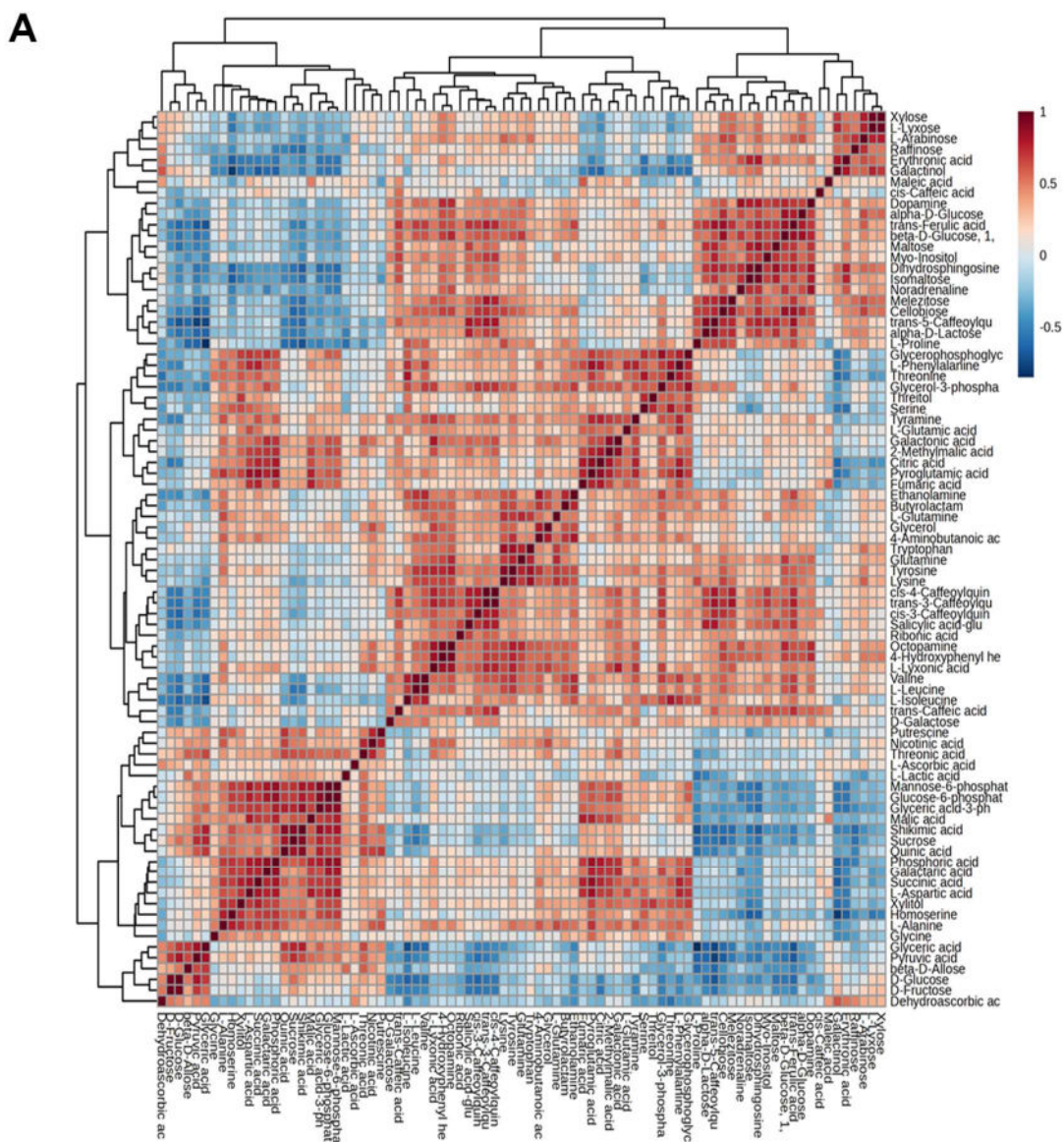
1178

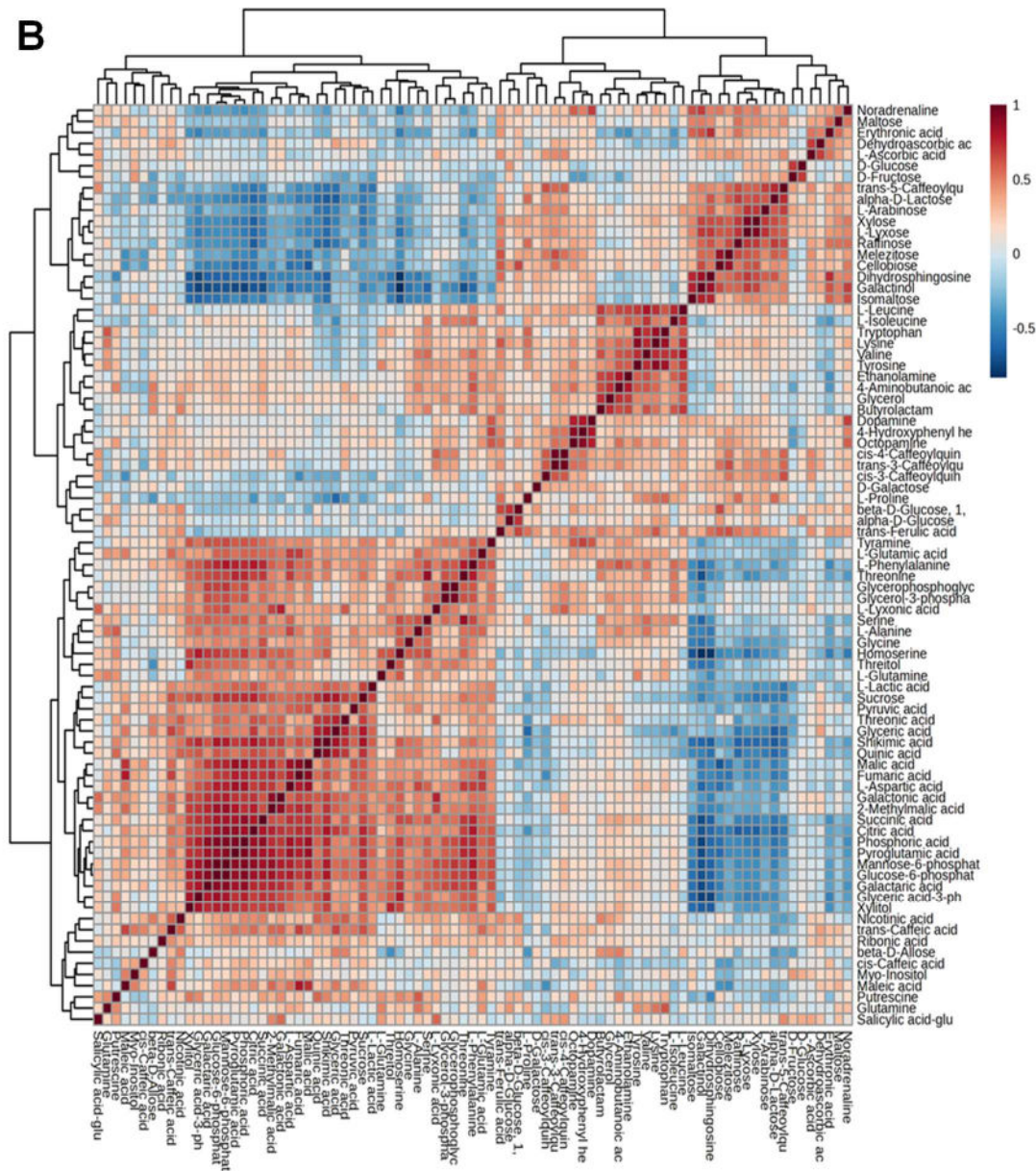
1179 **Fig. S1. Whole-canopy midday conductance (10:00–15:00).** Different letters above
1180 data points indicate statistically significant differences between genotypes ($p < 0.05$).



1181

1182 **Fig. S2. Pathway impact analysis** for WT and *stvinv* plants, with x-axis showing
1183 pathway impact (betweenness centrality) and y-axis showing significance ($-\log_{10}(p)$).





1186

1187 **Fig. S3. A-B Correlation heatmaps** reveal metabolic network organization in WT (E)

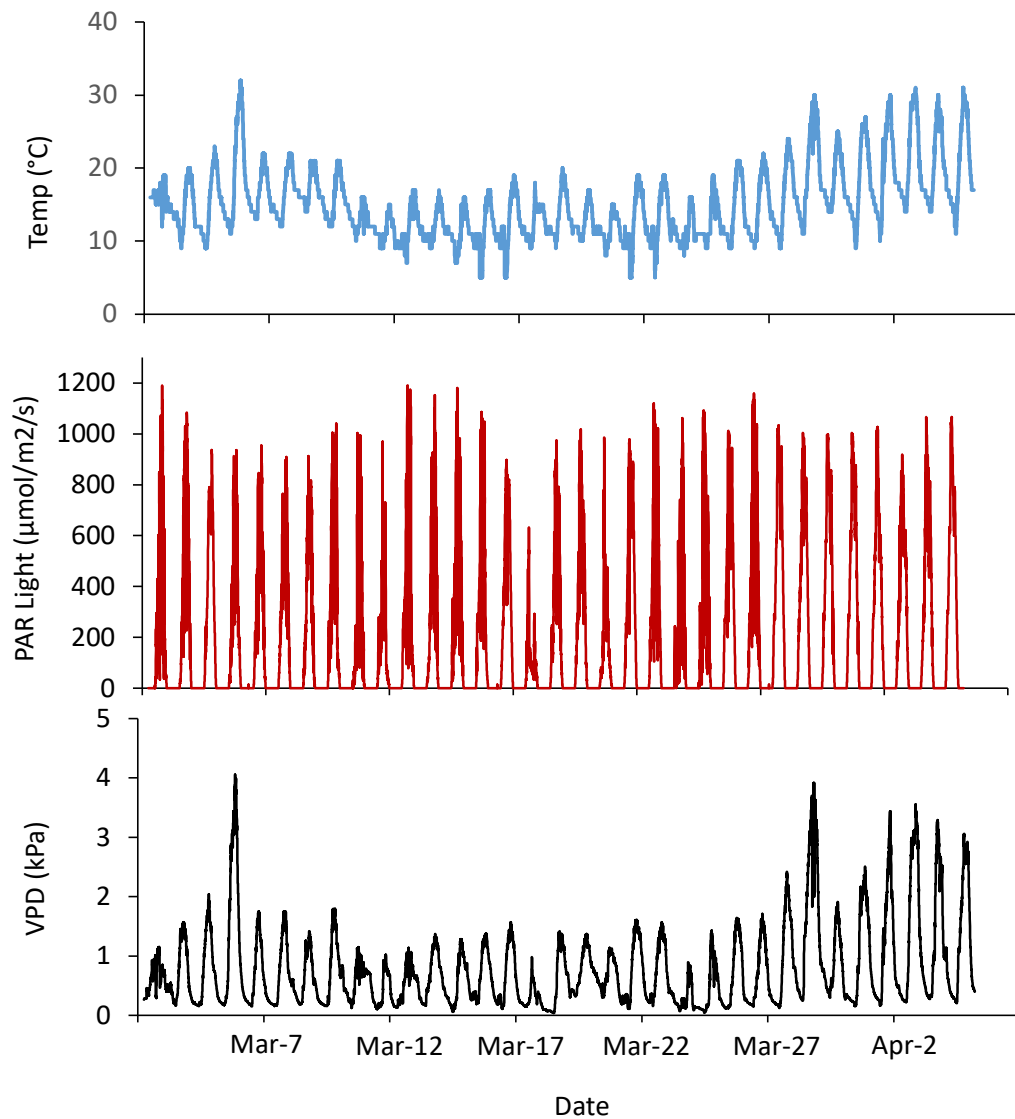
1188 and *stinv* plants (F). WT plants exhibit broad clustering among carbohydrate, amino

1189 acid, and secondary metabolites, reflecting a generalized stress response. In contrast,

1190 *stinv* plants show tight clustering of osmoprotective metabolites, such as sucrose,

1191 raffinose, and galactinol, indicating a focused metabolic adaptation to drought.

1192



1193

1194 **Fig. S4. Parameters of the soil–plant–atmosphere continuum monitored by**
1195 **“Plantarray”.** (A), air temperature (T, °C). (B), Photosynthetic active radiation (PAR,
1196 mmol m⁻² s⁻¹). (C), vapor pressure deficit (VPD, kPa). The data shown in the graph
1197 were obtained from the spring-season experiment in March - April 2022.